3

Review of Digital Filters

3.0 INTRODUCTION

This chapter includes a brief review of digital filter design techniques. Many of these topics are treated in Oppenheim and Schafer [1989]. Other related texts are [Rabiner and Gold, 1975], [Antoniou, 1979], and [Jackson, 1989]. Because of the availability of these references, our review is brief and limited to those techniques that are directly relevant to multirate systems. Discussions on relatively recent developments, for example eigenfilters (Section 3.2.3), and allpass decomposition of IIR filters (Section 3.6), are not available in the above references.

Some design techniques and structures will be treated in greater detail here. These include (a) the window design (FIR), (b) eigenfilters approach (FIR), (c) elliptic filters (IIR), (d) properties of allpass functions, and (e) allpass lattice structures. This elaboration is motivated by the applications in multirate filter bank design, as we indicate at the appropriate places.

Section 3.1 describes the common filter design specifications. In Sec. 3.2 and 3.3 we consider the design of finite impulse response (FIR) and infinite impules response (IIR) filters. Section 3.4 discusses allpass filters, which play a key role in the design of filter banks. Section 3.5 summarizes several special filters. In Sec. 3.6 we will show that many IIR filters (e.g., elliptic) can be expressed as a sum of two allpass filters. A special case of this (called IIR power symmetric filters) will find application in two-channel QMF bank design (Chap. 5).

3.1 FILTER DESIGN SPECIFICATIONS

The specifications on the magnitude response of a digital filter are usually given in terms of certain tolerances as demonstrated in Fig. 3.1-1(a) for the lowpass case. We assume the coefficients to be real, so only the region $0 \leq \omega \leq \pi$ has to be specified. Between the passband and stopband, we have to specify a transition band region since the response cannot change

abruptly from unity to zero. The region $0 \leq \omega \leq \omega_p$ is the passband and $\omega_S \leq \omega \leq \pi$ the stopband. The responses in the passband and stopband are required to lie within the tolerance regions.

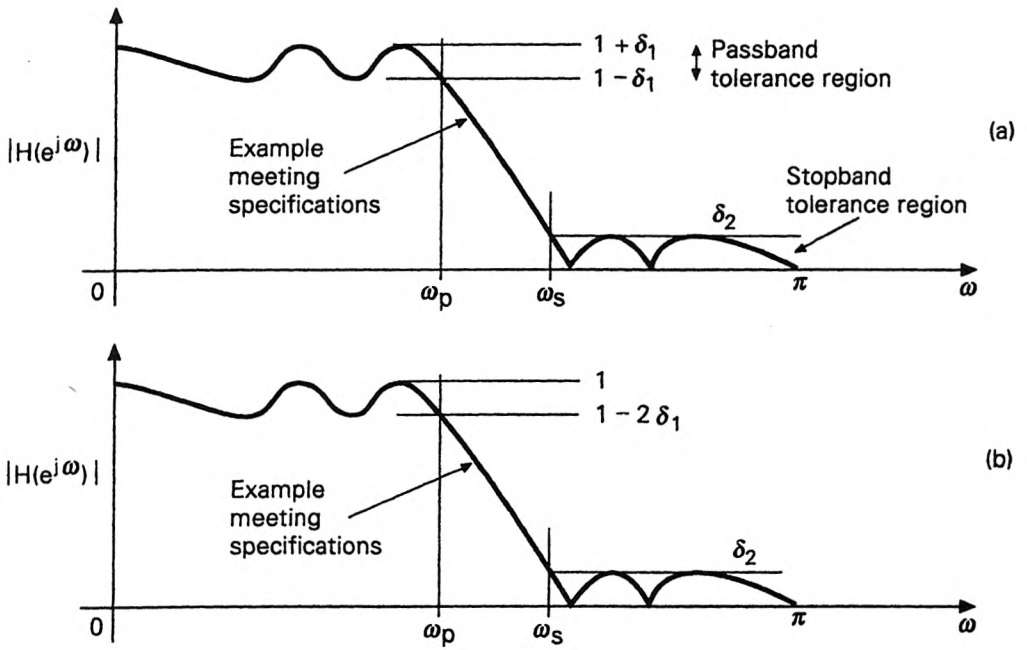

Figure 3.1-1 Magnitude response specifications for real-coefficient lowpass filters. (a) unnormalized magnitude, and (b) normalized magnitude.

The following terminology is standard.

$$\begin{aligned}
\delta_1 &= \text{peak passband ripple} \\
\delta_2 &= \text{peak stopband ripple} \\
A_S = -20\log_{10}\delta_2 &= \text{minimum stopband attenuation} \\
A_p = -20\log_{10}(1-\delta_1) &= \text{peak passband ripple in dB} \\
\omega_p &= \text{passband edge} \\
\omega_S &= \text{stopband edge} \\
\Delta\omega = \omega_S - \omega_p &= \text{transition BW (radians)} \\
\Delta f = \frac{\Delta\omega}{2\pi} &= \text{normalized transition BW (dimensionless).}
\end{aligned} \tag{3.1.1}$$

(Note that BW is an abbreviation for bandwidth.) The variable $f \triangleq \omega/2\pi$ is said to be the normalized frequency. Frequency response plots in the range

$0 \leq \omega \leq \pi$ correspond to the range $0 \leq f \leq 0.5$ in terms of f. Figure 3.1-1(a) also shows example of a response conforming to these specifications.

Normalized specifications. It is sometimes convenient to normalize the peak passband magnitude to unity. This can be done by dividing the response by $(1 + \delta_1)$. If $\delta_1 << 1$, this does not significantly affect the ripple sizes. Figure 3.1-1(b) shows this normalized set of specifications. One can verify that

$$A_p \approx 8.686\delta_1, \quad \text{for } \delta_1 << 1. \tag{3.1.2}$$

The quantity $\mathcal{A}(e^{j\omega}) = -20\log_{10}|H(e^{j\omega})|$ is said to be the attenuation characteristics for the filter. $-\mathcal{A}(e^{j\omega})$ is the magnitude response in dB. Fig. 3.1-2 shows how to specify the tolerances in terms of this quantity, for the case of normalized response. Note that the normalization of $|H(e^{j\omega})|$ corresponds to setting the minimum value of $\mathcal{A}(e^{j\omega})$ to 0 dB. The quantity A_{max} shown in this figure is called the *maximum passband attenuation.* With $\delta_1 << 1$, one can verify that

$$A_{max} = -20\log_{10}(1 - 2\delta_1) = 2A_p. \tag{3.1.3}$$

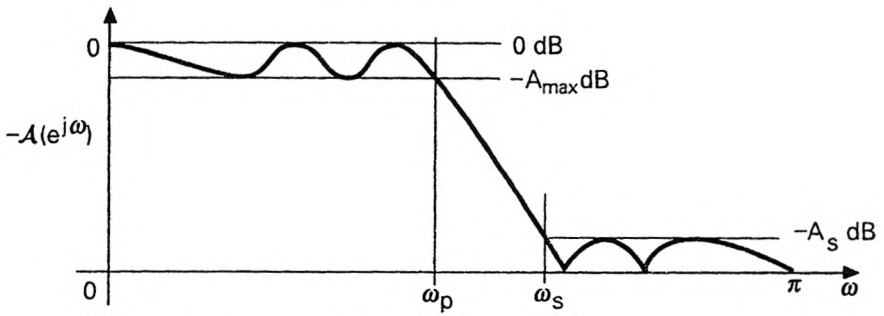

Figure 3.1-2 Specifications in terms of attenuation function, normalized to 0 dB. The attenuation goes to infinity at the transmission zeros.

Criteria for Optimality

We often talk about optimal filters, that is, filters that are "best" in some sense. The criterion of optimality has to be mentioned in order to make the meaning complete, as elaborated next.

Equiripple filters. For an equiripple filter, the extremal values of the error are the same throughout a given band. The examples in Fig. 3.1-1 are equiripple. To describe the optimality of such filters, let N denote the filter order, and let δ_1, δ_2 and Δf be defined as above. If any three of these four quantities are fixed, then the fourth parameter is minimum for an equiripple filter. Such a filter is said to be optimal in the *minimax* sense because, the *maximum* ripple sizes have been *minimized* for fixed N and Δf.

Least-squares filters. In the design of these filters, the square of the difference between the ideal and actual responses is integrated over the appropriate frequency bands and minimized. The simplest examples are FIR filters based on rectangular windows (Sec. 3.2). In Sec. 3.2.3 we will describe more useful variations, called *eigenfilters.*

Flatness constraints. In some applications it is desirable to have a high degree of flatness around zero frequency in the passband. Such flatness is usually specified in terms of the number of zeros of the derivative of $|H(e^{j\omega})|^2$ at $\omega = 0$. These specifications are called *flatness constraints.* In the IIR case, Butterworth filters (Sec. 3.3) serve this purpose. In the FIR case also it is possible to design filters with flatness constraints [Herrmann, 1971], and [Kaiser, 1979]. We will study this while discussing wavelet transforms in Chap. 11, where the flatness constraint is used to generate orthonormal basis functions with "regularity" properties.

3.2 FIR FILTER DESIGN

Consider Fig. 3.2-1(a) which shows an ideal lowpass response $H_i(e^{j\omega})$ with cutoff frequency ω_c, that is,

$$H_i(e^{j\omega}) = \begin{cases} 1 & |\omega| < \omega_c \\ 0 & \text{otherwise.} \end{cases} \tag{3.2.1}$$

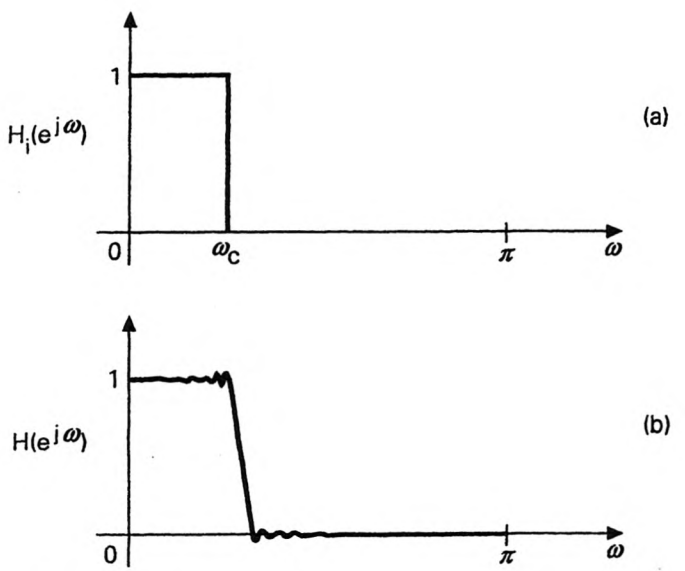

Figure 3.2-1 (a) The ideal lowpass response, and (b) truncated filter response.

So, this is a zero-phase filter with magnitude equal to unity in the passband and zero in the stopband (and no transition band whatsoever). Its impulse

response [inverse transform of $H_i(e^{j\omega})$] is given by

$$h_i(n) = \frac{\omega_c}{\pi}\left(\frac{\sin \omega_c n}{\omega_c n}\right), \quad -\infty \le n \le \infty. \tag{3.2.2}$$

It can be shown that this impulse response does not satisfy the BIBO stability requirement (Sec. 2.1.2). So, the ideal filter is not stable. In addition it is noncausal and IIR. No amount of delay would make the impulse response causal.

The simplest way to obtain an FIR lowpass filter from this would be to truncate the impulse response

$$h(n) = \begin{cases} h_i(n), & |n| \le N/2, \\ 0, & \text{otherwise.} \end{cases} \tag{3.2.3}$$

It can be shown (Problem 3.5) that the resulting response $H(e^{j\omega})$ approximates $H_i(e^{j\omega})$ in the least squares sense, that is, for a given N, $\int_0^{2\pi}[H_i(e^{j\omega}) - H(e^{j\omega})]^2 d\omega$ is minimized. (Note that both $H(e^{j\omega})$ and $H_i(e^{j\omega})$ are real.) However, the above truncation causes ripples in the passband and stopband [Fig. 3.2-1(b)], and the ripple size grows as we get closer to ω_c from either side. As N increases, the ripples get crowded closer to the cutoff frequency ω_c, but the size of the peak ripple does not decrease. This is called the *Gibbs phenomenon.* This is demonstrated in Fig. 3.2-2 where we show dB plots of the truncated response for $N = 20$ and $N = 50$. The minimum stopband attenuation A_S in both cases is only about 21 dB.

3.2.1 Window Design

An improvement over the truncation technique is offered by the use of windows. Here the impulse response is obtained as

$$h(n) = h_i(n)v(n), \tag{3.2.4}$$

where $v(n)$ is a window function, which is zero for $|n| > N/2$. As long as $v(n)$ is symmetric, we obtain a zero-phase filter $h(n)$ [since $h_i(n)$ is already symmetric]. If we set $v(n) = 1$ for $|n| \le N/2$ (rectangular window), windowing is equivalent to simple truncation.

In the frequency domain, the response $H(e^{j\omega})$ is a convolution of the ideal response $H_i(e^{j\omega})$ with $V(e^{j\omega})$. Two parameters of the window which control the quality of the filter response are: (a) the main lobe width ΔB of $V(e^{j\omega})$ which controls the filter transition bandwidth $\Delta\omega$, and (b) the peak sidelobe level of $V(e^{j\omega})$ which controls the peak passband and stopband ripples of $|H(e^{j\omega})|$. If the main lobe width of $V(e^{j\omega})$ is made smaller, the transition bandwidth of $H(e^{j\omega})$ is reduced. On the other hand, if the window has smaller side lobe ripples, the stopband attenuation provided by $H(e^{j\omega})$ is correspondingly improved. By appropriate choice of the window,

it is, therefore, possible to control both the attenuation and the transition bandwidth of the response $H(e^{j\omega})$.

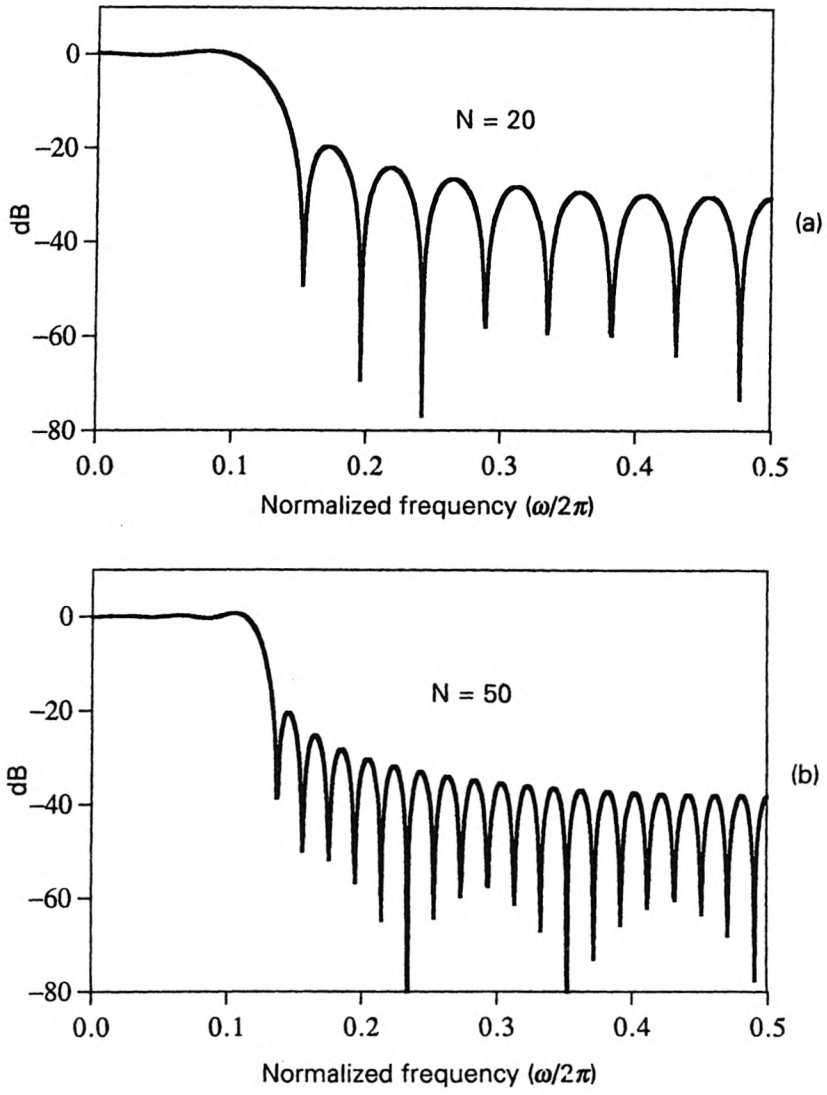

Figure 3.2-2 Magnitude responses obtained by truncation of the ideal impulse response.

Several windows have been invented (e.g., the Hamming window, Blackmann window, etc.), which offer various degrees of tradeoff between Δf and A_S [Oppenheim and Schafer, 1975]. A systematic way to obtain such a tradeoff is offered by the Kaiser window [Kaiser, 1974], which is actually a family of windows spanned by a parameter β. By adjusting β, one obtains

any desired stopband attenuation for $|H(e^{j\omega})|$; the order N is adjusted to satisfy the requirement on Δf. In all window-based methods, the resulting filter has $\delta_1 \approx \delta_2$.

The Kaiser window is given by

$$v(n) = \begin{cases} I_0\left[\beta\sqrt{1-\left(n/0.5N\right)^2}\right] \Big/ I_0(\beta), & -\frac{N}{2} \le n \le \frac{N}{2}, \\ 0 & \text{otherwise}, \end{cases} \tag{3.2.5}$$

where $I_0(x)$ is the modified zeroth-order Bessel function, which can be computed from the power series

$$I_0(x) = 1 + \sum_{k=1}^{\infty} \left[\frac{(0.5x)^k}{k!}\right]^2. \tag{3.2.6}$$

Note that $I_0(x)$ is positive for all (real) x. In most practical designs, only about twenty terms in the above summation need to be retained. Once $v(n)$ is computed in this manner, the coefficients of the filter can be found from (3.2.4) where $h_i(n)$ is as in (3.2.2) (with $\omega_c = 0.5(\omega_p + \omega_S)$). The filter order is evidently equal to N. Since $v(n)$ and $h_i(n)$ are even functions of n, the resulting FIR filter $h(n)$ has zero phase.

The parameter β depends on the attenuation requirements of the lowpass filter. Kaiser has developed simple formulas for estimating the parameters β and N, for given A_S and Δf. The quantity β is found from

$$\beta = \begin{cases} 0.1102(A_S - 8.7) & \text{if } A_S > 50 \\ 0.5842(A_S - 21)^{0.4} + 0.07886(A_S - 21) & \text{if } 21 < A_S < 50 \\ 0 & \text{if } A_S < 21. \end{cases} \tag{3.2.7}$$

Given the quantities A_S and Δf, the filter order N is estimated from

$$N \approx \frac{A_S - 7.95}{14.36\Delta f}. \tag{3.2.8}$$

Notice that once β and N are determined, we do not have independent control over δ_1. In most designs, the resulting δ_1 comes out to be very close to δ_2 (which in turn is determined by A_S).

It has been demonstrated [Saramaki, 1989] that the Kaiser window can also be obtained from a rectangular window by means of a change of variables.

Design Example 3.2.1: FIR Lowpass Filter Using Kaiser Window

Suppose the design specifications are $\omega_p = 0.2\pi, \omega_S = 0.3\pi$, $A_S = 40$dB, and $\delta_1 = \delta_2$. (The value of A_S implies $\delta_2 = 0.01$.) The estimated values of β and N are $\beta = 3.395, N = 44.6$. The order can be rounded off to the next

even integer, that is, $N = 46$. (This makes $N/2$ even in (3.2.5).) The cutoff frequency $\omega_c = 0.5(\omega_p + \omega_S) = 0.25\pi$.

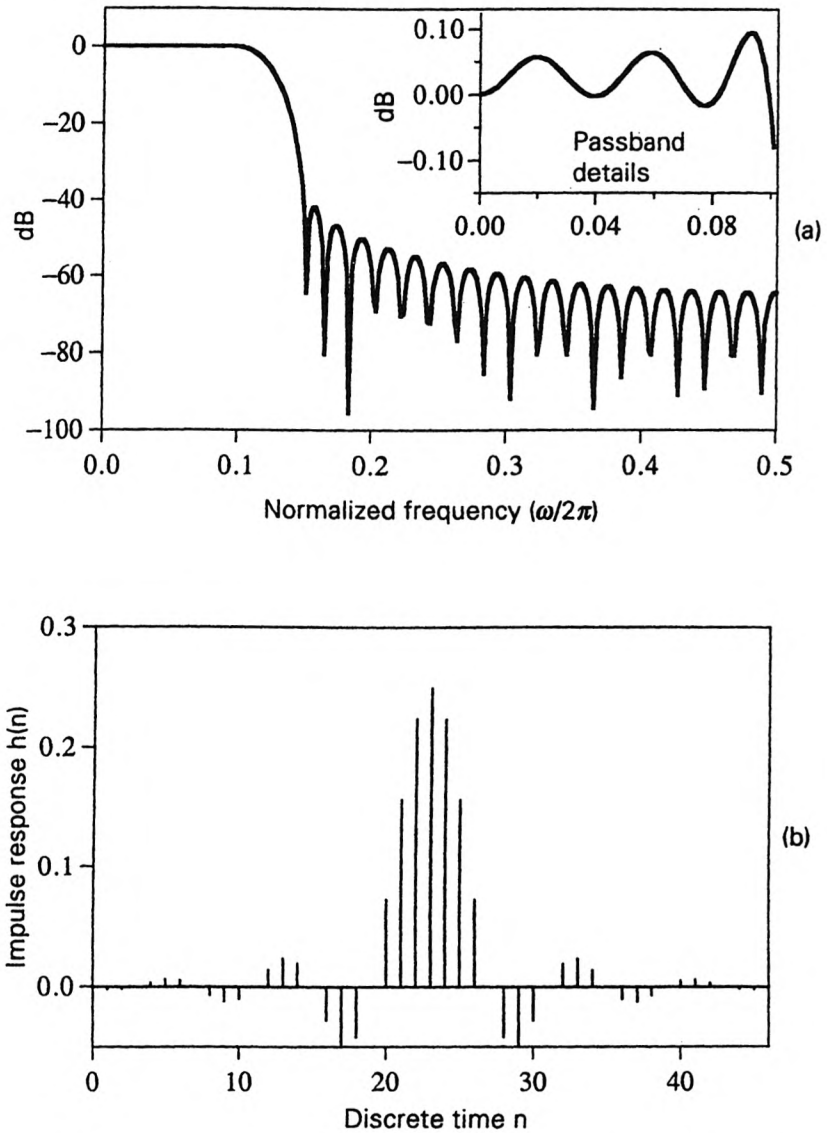

Figure 3.2-3 Design example 3.2.1. Lowpass filter based on Kaiser window. (a) Magnitude response, and (b) impulse response.

We can now compute the coefficients of $v(n)$ and $h_i(n)$ as above, and obtain $h(n)$ from (3.2.4). Fig. 3.2-3(a) shows the magnitude response plot (with $N = 46$) which meets the required specifications. For clarity, the passband details are shown separately in magnified form. One can verify

that the peak ripple δ_1 is very close to δ_2, that is, $\delta_1 \approx 0.01$. Part (b) of the figure shows the impulse response coefficients.

Summary. The Kaiser window technique offers a very simple means of designing linear phase FIR filters. No elaborate optimization steps are involved. The quantities ω_p, ω_S, and δ_2 can be specified independently, but not δ_1 (which turns out to be close to δ_2). The windowing technique is not suitable for design of filters with more sophisticated specifications (such as unequal ripple sizes, nonconstant passband responses, and so on).

The Dolph-Chebyshev Function: An Optimal Window

The Dolph-Chebyshev (DC) window $v(n)$ has the property that the *max*imum side lobe level of $|V(e^{j\omega})|$ is *min*imized in the region $\sigma \leq \omega \leq \pi$. Consequently, this is called a *minimax window.* The plot of $|V(e^{j\omega})|$ is equiripple in the region $\sigma \leq \omega \leq \pi$. For this window a closed form expression in the frequency domain, based on Chebyshev polynomials, is available. This can be found in Helms [1971]. The window coefficients in the time domain can be found by performing an inverse Fourier transform. Details are omitted.

3.2.2 The Prolate Sequence: Another Optimal Window

The Kaiser window is a good approximation to a class of optimal windows called *prolate spheroidal* (or just prolate) wave sequences $v(n)$ [Slepian, 1978]. A prolate sequence is a real sequence of finite length $N+1$ and unit energy, with the energy in the frequency region $\sigma \leq \omega \leq \pi$ minimized. The quantities N and σ can be regarded as parameters of the prolate sequence family. In all our discussions we assume $0 < \sigma < \pi$.

We now show how the optimal window coefficients can be computed. This makes use of some results from matrix theory (especially Rayleigh's principle), reviewed in Appendix A. The derivation will show how we can pass from optimal *windows* to optimal (least squares) *filters* (Sec. 3.2.3).

Matrix-vector Formulation of the Optimization Problem

Assume $v(n)$ is causal with length $N+1$ so that $V(z) = \sum_{n=0}^{N} v(n) z^{-n}$. Define

$$\phi_S \triangleq \int_{\sigma}^{\pi} |V(e^{j\omega})|^2 \frac{d\omega}{\pi}. \tag{3.2.9}$$

This is the quantity to be minimized under the unit-energy constraint. Because of Parseval's theorem we can write the constraint either in the time domain or in the frequency domain:

$$\int_0^{\pi} |V(e^{j\omega})|^2 \frac{d\omega}{\pi} = 1 \quad \text{or} \quad \sum_{n=0}^{N} v^2(n) = 1. \tag{3.2.10}$$

[Remember $v(n)$ is real.] Fig. 3.2-4 demonstrates the idea: we minimize the area of the shaded region, for a fixed total area under the curve. Minimizing

ϕ_S under the constraint (3.2.10) is equivalent to maximizing

$$\phi \triangleq \int_0^{\sigma} |V(e^{j\omega})|^2 \frac{d\omega}{\pi}. \tag{3.2.11}$$

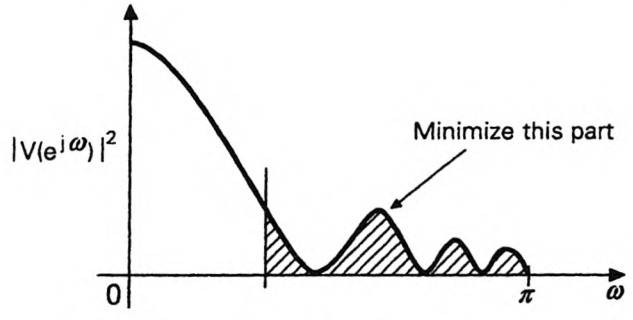

Figure 3.2-4 Design of the optimal window.

Defining the vectors

$$\mathbf{v} = [\,v(0) \quad v(1) \quad \ldots \quad v(N)\,]^T, \quad \mathbf{e}(z) = [\,1 \quad z^{-1} \quad \ldots \quad z^{-N}\,]^T, \tag{3.2.12}$$

we have $V(e^{j\omega}) = \mathbf{v}^\dagger(n)\mathbf{e}(e^{j\omega})$ so that

$$|V(e^{j\omega})|^2 = V(e^{j\omega})V^*(e^{j\omega}) = \mathbf{v}^\dagger \mathbf{e}(e^{j\omega})\mathbf{e}^\dagger(e^{j\omega})\mathbf{v}. \tag{3.2.13}$$

(We could have used $\mathbf{v}^T$ instead of $\mathbf{v}^\dagger$ since $\mathbf{v}$ is real; we will use $\mathbf{v}^\dagger$ for notational uniformity). We can rewrite the objective function ϕ as

$$\phi = \mathbf{v}^\dagger \Big[\int_0^{\sigma} \mathbf{R}(\omega)\frac{d\omega}{\pi}\Big]\mathbf{v}, \tag{3.2.14}$$

where

$$\mathbf{R}(\omega) \triangleq \mathbf{e}(e^{j\omega})\mathbf{e}^\dagger(e^{j\omega}). \tag{3.2.15}$$

The $(N+1)\times(N+1)$ matrix $\mathbf{R}(\omega)$ has (m,n) element

$$e^{-j(m-n)\omega} = \cos(m-n)\omega - j\sin(m-n)\omega, \tag{3.2.16}$$

so that $\mathbf{R}(\omega)$ is Hermitian. Its imaginary part $\mathbf{Q}(\omega)$ is therefore antisymmetric. So, $\mathbf{v}^\dagger\mathbf{Q}(\omega)\mathbf{v} = 0$ (since $\mathbf{v}$ is real). Thus, ϕ can be simplified to

$$\phi = \mathbf{v}^\dagger \mathbf{P}\mathbf{v}, \tag{3.2.17}$$

where $\mathbf{P}$ has (m,n)th entry

$$p_{mn} = \int_0^{\sigma} \cos(m-n)\omega\frac{d\omega}{\pi} = \frac{\sin(m-n)\sigma}{(m-n)\pi}, \quad 0 \le m,n \le N. \tag{3.2.18}$$

The unit-energy constraint (3.2.10) can also be rewritten in terms of $\mathbf{v}$ as

$$\mathbf{v}^\dagger \mathbf{v} = 1, \tag{3.2.19}$$

that is, $\mathbf{v}$ has unit norm. Summarizing, the problem of finding the unit-energy window function $v(n)$ with smallest energy in $\sigma \leq \omega \leq \pi$ has been converted to the problem of finding a unit-norm vector $\mathbf{v}$ which maximizes (3.2.17).

Solution to the Optimization Problem

Now the matrix $\mathbf{P}$ is evidently real and symmetric (so it is Hermitian). From Rayleigh's principle (Appendix A) we know that all the eigenvalues of $\mathbf{P}$ are real, and that ϕ is maximized under the constraint (3.2.19) if, and only if, $\mathbf{v}$ is an eigenvector corresponding to the largest eigenvalue λ_N. We can therefore compute the coefficients of the optimal window $v(n)$ simply by computing this eigenvector. There exist standard techniques such as the power-method (Appendix A) for this computation. The eigenvalue λ_N is the quantity (3.2.11) after maximization, and satisfies $\lambda_N < 1$ [in view of (3.2.10)].

Design Example 3.2.2: Optimal Window

As an example, let $\sigma = 0.1\pi$ and $N = 32$. The optimum window computed in the above manner has response shown in Fig. 3.2-5 which also shows the Kaiser window response with same N, and $\beta = 4.55$. The agreement between the plots demonstrates that the Kaiser window is an excellent approximation to the optimal window. The parameter σ of the optimal window has the same role as the tradeoff parameter β of the Kaiser window. It is intuitively clear that if we increase σ, then the optimum window has smaller peak side lobe level. This is indeed the case as one can verify by plotting $|V(e^{j\omega})|$ for different values of σ.

Notice that there are precisely 16 transmission zeros of $V(e^{j\omega})$ in the range $\sigma \leq \omega < \pi$, that is, a total of 32 on the unit circle. More generally, the optimal window always has all zeros on the unit circle. This is a consequence of the properties of $\mathbf{P}$, as will be elaborated.

Properties of P

The quantity ϕ is the energy of the window in the region $0 \leq |\omega| \leq \sigma$ and cannot be zero for $\sigma > 0$. This statement is true for any nonzero $v(n)$, hence any nonzero $\mathbf{v}$. In other words, $\mathbf{P}$ is positive definite for any $\sigma > 0$. It is also clear from (3.2.18) that $\mathbf{P}$ is Toeplitz (Appendix A). So, $\mathbf{P}$ is real, symmetric, positive definite and Toeplitz.

Denote the eigenvalues of $\mathbf{P}$ by λ_i, $0 \leq i \leq N$. We have $\lambda_i > 0$ due to positive definiteness. Combining with $\lambda_N < 1$, we get

$$0 < \lambda_0 \leq \lambda_1 \leq \ldots \leq \lambda_N < 1. \tag{3.2.20}$$

Less obvious is the fact [Slepian, 1978] that the above inequalities are strict, that is, $\lambda_i < \lambda_{i+1}$. This means that the eigenvectors are unique (up to scale) so that, in particular, the optimal window $\mathbf{v}$ is unique.

Zeros of the window. Based on this uniqueness, one can show (Problem 3.6) that all the zeros of the optimal window $V(z)$ lie on the unit circle. This implies, in turn, that $v(n)$ is a symmetric sequence, that is, $v(n) = v(N-n)$. [It cannot be antisymmetric, as it would mean $V(e^{j0}) = 0$.] Redefining $v(n)$ to be $v(n+M)$, where $M = N/2$, we obtain the zero-phase optimal window which can now be used in (3.2.4) to design $h(n)$. The filter is guaranteed to have linear phase because of the symmetry of $v(n)$.

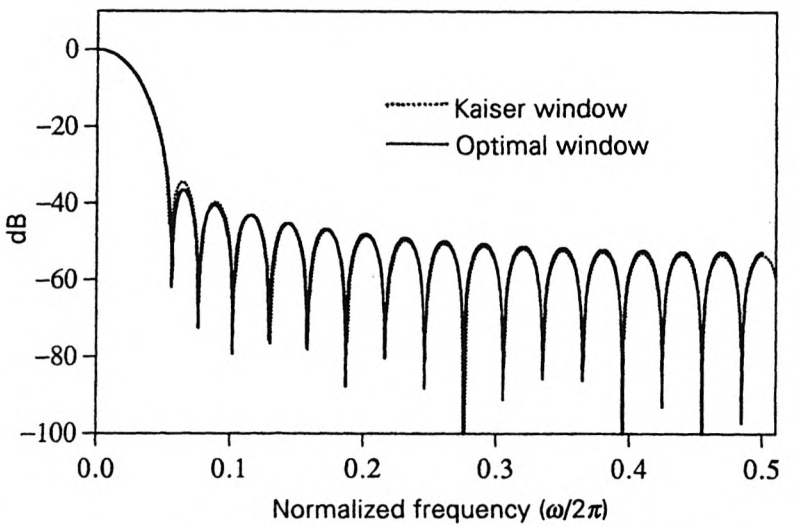

Figure 3.2-5 Design example 3.2.2. Responses of the optimal window and the Kaiser window.

3.2.3 Optimal Lowpass Eigenfilters

As discussed in Sec. 3.1, there are several classes of optimal filters, according to the choice of the performance measure (or objective function) to be minimized. In general, FIR filters based on the window approach do not yield filters which are optimal in any sense, even if the window is optimal in some sense.

An exception is the rectangular window which yields a filter $H(e^{j\omega})$ which is optimal in the least squares sense, that is, the integral

$$\int_0^{2\pi} |H_i(e^{j\omega}) - H(e^{j\omega})|^2 \, d\omega$$

is minimized, where $H_i(e^{j\omega})$ is the ideal response (3.2.1) (see Problem 3.5). These filters, however, suffer from Gibbs phenomenon as seen earlier. Fur-

thermore, the above integral includes the transition band error, which should actually be excluded.

In this section, we introduce lowpass *eigenfilters* [Vaidyanathan and Nguyen, 1987a]. These are optimal in the least squares sense but the objective function itself is defined differently, by formulating it as a sum of the passband and stopband errors. The error of approximation in the transition band is not included. Such an objective function is obtained by adding a second term to (3.2.9), which was used to design an optimal window. The second term represents a 'squared measure' of the deviation from the ideal passband response. The formulation is such that we can obtain the optimal filter coefficients from an eigenvector of an appropriate matrix.

The eigenfilter approach is different from other types of least squares approaches for FIR design, which are obtainable by matrix inversion, for example, the one described in Roberts and Mullis [1987, Sec. 7.2].

Why eigenfilters? One of the advantages of eigenfilters over other FIR filters (such as equiripple filters) is that, they can be designed to incorporate a wide variety of time domain constraints such as the step response constraint, Nyquist constraint and so on, in addition to the usual frequency domain requirements. The filter coefficients are obtained simply by computing an eigenvector of a positive definite matrix, which is derived from the time and frequency domain specifications. Eigenfilters can be used for optimal design of the so-called Nyquist filters, which are ideally suited for interpolation filtering (Chap. 4). Nyquist filters also find use in filter bank design.

To introduce the basic idea of eigenfilters, consider Type 1 linear phase filters (Table 2.4.1). These have the form $H(z) = \sum_{n=0}^{N} h(n)z^{-n}$, where $h(n)$ is real and satisfies $h(n) = h(N-n)$. Moreover N is even. The amplitude response is

$$H_R(\omega) = \sum_{n=0}^{M} b_n \cos \omega n = \mathbf{b}^T \mathbf{c}(\omega), \tag{3.2.21}$$

where $M = N/2$ and

$$\mathbf{b} = [\, b_0 \quad b_1 \quad \dots \quad b_M \,]^T, \quad \mathbf{c}(\omega) = [\, 1 \quad \cos\omega \quad \dots \quad \cos M\omega \,]^T \tag{3.2.22}$$

The aim is to find the coefficients $\mathbf{b}$ such that an appropriate objective function is minimized. The objective function should reflect the stopband energy (energy in $\omega_S \leq \omega \leq \pi$) as well as the passband accuracy. We will formulate the minimization problem in such a way that the optimal $\mathbf{b}$ can be computed as an eigenvector of an appropriate positive definite matrix.

Since $H(e^{j\omega}) = e^{-j\omega M} H_R(\omega)$ we have

$$|H(e^{j\omega})|^2 = H_R^2(\omega) = \mathbf{b}^T \mathbf{c}(\omega)\mathbf{c}^T(\omega)\mathbf{b}. \tag{3.2.23}$$

So the stopband energy is

$$E_S = \int_{\omega_S}^{\pi} |H(e^{j\omega})|^2 \frac{d\omega}{\pi} = \mathbf{b}^T \mathbf{P} \mathbf{b} \tag{3.2.24}$$

where

$$\mathbf{P} = \int_{\omega_S}^{\pi} \mathbf{c}(\omega)\mathbf{c}^T(\omega)\frac{d\omega}{\pi}.$$

The (m,n) element of $\mathbf{P}$ is

$$p_{mn} = \int_{\omega_S}^{\pi} \cos(m\omega)\cos(n\omega)\frac{d\omega}{\pi} \tag{3.2.25}$$

which can be evaluated in terms of ω_S, m, and n. The passband error can be included in the objective function as follows. The amplitude response at zero frequency is given by $H_R(0) = \mathbf{b}^T\mathbf{1}$, where $\mathbf{1}$ is the vector of all 1's. By taking this as a reference, the passband deviation at any frequency can be written as

$$\mathbf{b}^T\mathbf{1} - \mathbf{b}^T\mathbf{c}(\omega) = \mathbf{b}^T\big[\mathbf{1} - \mathbf{c}(\omega)\big], \tag{3.2.26}$$

so that the quantity

$$E_p = \mathbf{b}^T\mathbf{Q}\mathbf{b} \tag{3.2.27}$$

is a measure of mean square passband error, where

$$\mathbf{Q} = \int_0^{\omega_p} [\mathbf{1} - \mathbf{c}(\omega)][\mathbf{1} - \mathbf{c}(\omega)]^T\frac{d\omega}{\pi}. \tag{3.2.28}$$

Now define the objective function

$$\phi = \alpha E_S + (1-\alpha)E_p, \tag{3.2.29}$$

where $0 < \alpha < 1$. Here α is a tradeoff parameter between passband and stopband performances. We then have

$$\phi = \mathbf{b}^T\mathbf{R}\mathbf{b}, \tag{3.2.30}$$

where

$$\mathbf{R} = \alpha\mathbf{P} + (1-\alpha)\mathbf{Q}. \tag{3.2.31}$$

It is easily verified that $\mathbf{R}$ is a real, symmetric and positive definite matrix (Problem 3.8). The unit-norm vector $\mathbf{b}$ which mimimizes ϕ is the eigenvector corresponding to the minimum eigenvalue λ_0 of $\mathbf{R}$, and can be calculated using the 'power method' described in Sec. A.8, Appendix A.

Design Example 3.2.3. Linear Phase Eigenfilters.

Consider an example with bandedges $\omega_p = 0.3\pi, \omega_S = 0.5\pi$, and order $N = 30$. Fig. 3.2-6 shows the magnitude responses of the eigenfilters designed as above, for two values of α. The passband details are also shown separately. It is clear that as α is increased the peak stopband ripple is reduced at the expense of peak passband ripple.

Even though the role of the tradeoff parameter α is very clear, there is no known analytical relation between α and the relative peak ripple sizes δ_1 and δ_2.

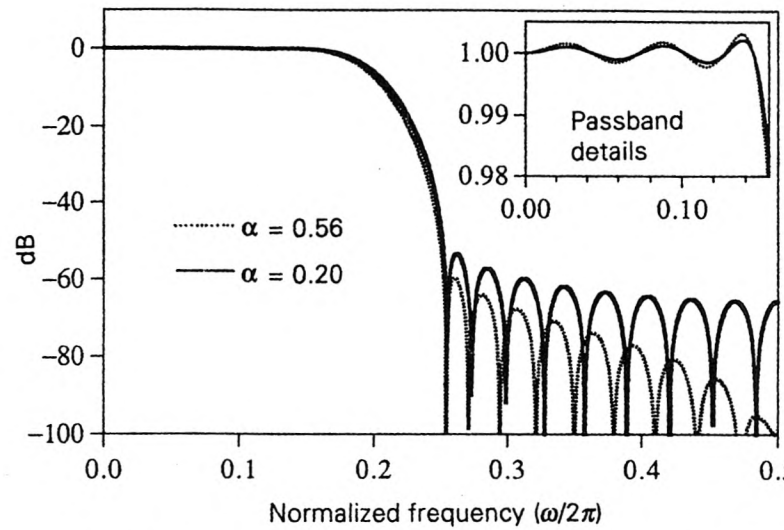

Figure 3.2-6 Design example 3.2.3. Magnitude response plots for linear phase eigenfilters.

Extensions of the eigenfilter approach. The approach is readily extended to the case of other types of filters such as highpass and bandpass filters, differentiators, and Hilbert transformers [Pei and Shyu, 1989]. It is also possible to extend the method to include certain *flatness* constraints in the passband. Finally, extensions to the case of two dimensional filters have also been made. These extensions permit faster design of two dimensional FIR filters than most other methods. See Nashashibi and Charalambous [1988], and Pei and Shyu [1990].

3.2.4 Equiripple FIR Filters

The filters which result from the Kaiser window approach, and the eigenfilter approach are such that the ripple size grows as we move closer to the band edge. Because of this, the filter performace exceeds (i.e., is better than the specifications) for most frequencies except around ω_p and ω_S. So, the filter has actually been overdesinged in this sense. If this can be avoided, it is possible to reduce N while meeting the same set of specifications. The way to achieve this is to distribute the approximation error uniformly in the passband (and also in the stopband). This leads to the idea of equiripple FIR filters (Fig. 3.2-7). Here all the local extrema of the approximation error in the passband are equal. The same is true in the stopband.

For a given set of specifications ω_p, ω_s, δ_1, and δ_2 it turns out that an equiripple filter has the smallest possible order N. A more precise state-

ment of optimality is given by the so-called 'alternation theorem' [Rabiner and Gold, 1975]. Based on this theorem, the problem of designing equiripple linear phase filters has been solved, by using a technique called the *Remez exchange algorithm.* The resulting algorithm [Parks and McClellan, 1972], often referred to as the McClellan-Parks algorithm, permits unequal ripple sizes in each of the frequency bands (unlike the window techniques). We skip details here. Suffice it to say that the method is very systematic, and permits one to design a large family of linear phase FIR filters (all four Types in Table 2.4.1.) including differentiators and Hilbert transformers. Special requirements such as time domain constraints and flatness constraints cannot, however, be incorporated in a straightforward manner.

Estimating the filter order. Several formulas have been proposed for estimating the order of a linear phase equiripple lowpass filter with specifications $\omega_p, \omega_S, \delta_1, \delta_2$. The most well known of these are:

$$N = \begin{cases} \dfrac{-20\log_{10}\sqrt{\delta_1\delta_2} - 13}{14.6\Delta f} & \text{(Kaiser's formula)} \\ \dfrac{2\ \log_{10}(\frac{1}{10\delta_1\delta_2})}{3\Delta f} & \text{(Bellanger's formula),} \end{cases} \tag{3.2.32}$$

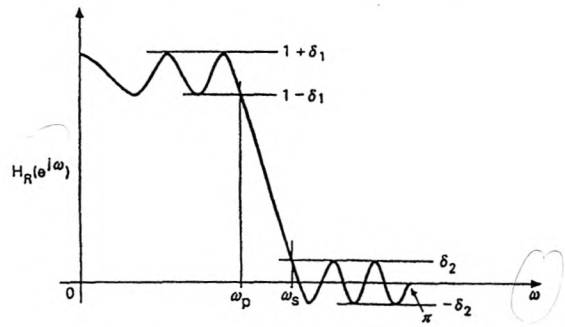

Figure 3.2-7 An equiripple amplitude response.

where $\Delta f = (\omega_S - \omega_p)/2\pi$. Notice the simplicity of these formulas. They also clearly reveal the nature of dependency of N on the ripple sizes and Δf. A more accurate (but not as simple) formula has been reported by Herrmann, and can be found in Rabiner, et al. [1975].

3.2.5 Spectral Factorization

In some filter design problems, one finds it necessary to compute a spectral factor (defined below) of a transfer function. An example is in the design of FIR QMF banks (Chap. 5). We now describe the basic idea.

Let $H(z) = \sum_{n=-M}^{M} h(n)z^{-n}$ be a zero-phase FIR transfer function so that $H(e^{j\omega})$ is real. If in addition $H(e^{j\omega}) \geq 0$ for all ω, we can factorize it as $H(e^{j\omega}) = |H_0(e^{j\omega})|^2$. That is, we can write

$$H(z) = \widetilde{H}_0(z)H_0(z), \tag{3.2.33}$$

where $H_0(z)$ is causal FIR with order M, that is, $H_0(z) = \sum_{n=0}^{M} h_0(n)z^{-n}$. The filter $H_0(z)$ is said to be a spectral factor of $H(z)$. [The notation $\widetilde{H}_0(z)$ is described in Sec. 2.3.]

To see how $H_0(z)$ can be identified, recall that the zero-phase property of $H(z)$ implies that, if z_k is a zero then so is $1/z_k^*$. The property $H(e^{j\omega}) \geq 0$, on the other hand, implies that if z_k is on the unit circle, then it is a zero of even multiplicity (e.g., a double zero). Fig. 3.2-8 shows a typical set of zeros of the function $H(z)$. Once these zeros are known, we can obtain $H_0(z)$ by assigning to it the zero located at either z_k or $1/z_k^*$, for each k. The figure demonstrates this. If z_k is assigned to $H_0(z)$, then $1/z_k^*$ is assigned to $\widetilde{H}_0(z)$. We can write $H_0(z)$ as

$$H_0(z) = c \prod_{k=1}^{M} (1 - z^{-1}z_k), \tag{3.2.34}$$

so that

$$\widetilde{H}_0(z) = c^* \prod_{k=1}^{M} (1 - zz_k^*). \tag{3.2.35}$$

Equation (3.2.33) can now be satisfied for appropriate constant c.

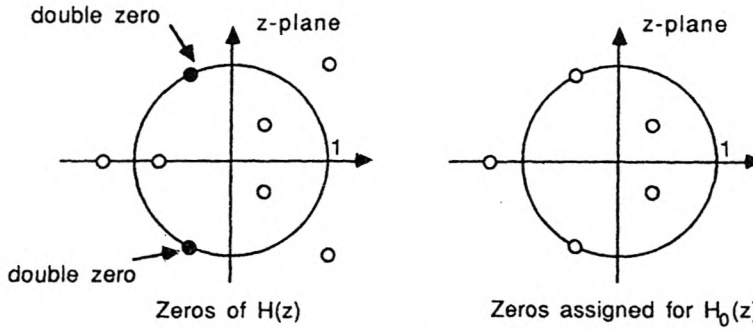

Figure 3.2-8 Obtaining a spectral factor of a transfer function $H(z)$.

Nonuniqueness. The spectral factor $H_0(z)$ is in general not unique because we can replace a particular factor $(1 - z^{-1}z_k)$ in $H_0(z)$ with $(1 - z^{-1}/z_k^*)$ (and readjust c) so that (3.2.33) continues to hold. In other words, if we replace a zero z_k of $H_0(z)$ with $1/z_k^*$, the result continues to be a spectral factor after scaling. If $H(z)$ happens to have all zeros on the unit circle, then the spectral factor is unique (up to a scale factor of unit-magnitude). If we choose all zeros such that they satisfy $|z_k| \leq 1$ (or $|z_k| \geq 1$) then we have a minimum (or maximum) phase spectral factor. Such a spectral factor is unique (up to a scale factor of unit magnitude). If $H(z)$ is free from unit-circle zeros, then these become strictly minimum (or maximum)

phase factors. Finally, note that if the zero-phase function $H(e^{j\omega})$ is an even function of ω, then $h(n)$ is real. In this case we can find $H_0(z)$ with real coefficients; in particular we can find minimum or maximum phase spectral factors with real coefficients.

The most obvious technique to compute a spectral factor is to find the $2M$ zeros of $H(z)$ and pick an appropriate subset of M zeros to define $H_0(z)$. There exist more efficient procedures, which do not compute the zeros of $H(z)$ [Mian and Nainer, 1982], and [Friedlander, 1983]. One such procedure is described in Appendix D.

Application in Nonlinear Phase FIR Design

In some applications linearity of phase is not particularly important, even though FIR filters are still preferred for other reasons. This situation arises, for example, in one dimensional QMF banks and will be discussed in Chap. 5. In general, by relaxing the linear phase property, it is possible to reduce the filter order required for a given set of magnitude response specifications. We now describe a technique [Herrmann and Schüssler, 1970], for designing nonlinear phase FIR filters.

Let $G(z) = \sum_{n=-M}^{M} g(n)z^{-n}$ be a zero phase FIR filter designed using any one of the techniques described above. Let δ_2 denote the peak stopband ripple. Now consider the filter

$$H(z) = G(z) + \delta_2. \tag{3.2.36}$$

The impulse response of $H(z)$ is given by

$$h(n) = \begin{cases} g(n) & n \neq 0 \\ g(n) + \delta_2 & n = 0. \end{cases} \tag{3.2.37}$$

The frequency response of $H(z)$ is

$$H(e^{j\omega}) = G(e^{j\omega}) + \delta_2. \tag{3.2.38}$$

Since $G(z)$ has zero phase, $G(e^{j\omega})$ is real, so that $H(e^{j\omega})$ is obtained just by lifting the response $G(e^{j\omega})$ by δ_2. This is demonstrated in Fig. 3.2-9 for the equiripple case. It is clear that $H(e^{j\omega}) \geq 0$ for all ω, so that we can find a spectral factor $H_0(z)$ of $H(z)$ (as demonstrated in Fig. 3.2-8). In particular if $G(z)$ has real coefficients, then so does $H_0(z)$. The spectral factor $H_0(z)$ in general does not have linear phase. As explained above it is possible to find a minimum or maximum phase (or even a mixed phase) spectral factor.

Suppose we wish to design a minimum phase equiripple FIR filter $H_0(z)$ with bandedges ω_p, ω_S, and peak ripples ϵ_1, and ϵ_2. We then design a zero phase filter $G(z)$ with same bandedges ω_p and ω_S but with ripples as follows:

$$\begin{aligned} \text{peak to peak passband ripple } 2\delta_1 &\approx 1 - (1 - 2\epsilon_1)^2 \\ \text{peak stopband ripple } \delta_2 &= \epsilon_2^2/2. \end{aligned} \tag{3.2.39}$$

We can now obtain $H(z) = G(z) + \delta_2$ and compute the minimum-phase spectral factor $H_0(z)$.

Notice that the stopband attenuation of $G(z)$ is more than twice that of $H_0(z)$. For example suppose $H_0(z)$ requires a stopband attenuation of 60 dB. Then $H(z)$ has stopband attenuation 120 dB and $G(z)$ has 126 dB. Spectral factorization of systems with such large attenuation is typically subject to considerable numerical error, particularly if the procedure involves the computation of zeros of $H(z)$.

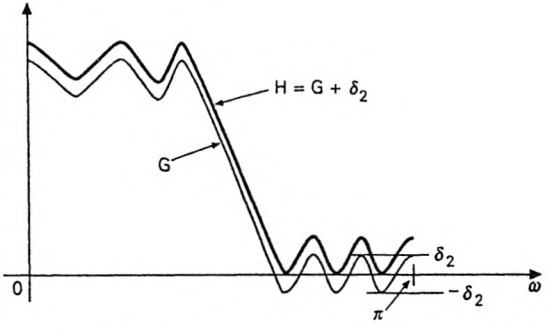

Figure 3.2-9 Lifting the amplitude response of a zero-phase filter $G(z)$ to obtain $H(z)$ with nonnegative amplitude response.

3.3 IIR FILTER DESIGN

The most striking advantage of FIR filters is that they can be designed to have exact linear phase. In situations where linearity of phase is not important, it is sometimes preferable to use IIR filters because an IIR filter usually requires a much lower order for the same set of magnitude response specifications. (See Design Example 3.3.2 later). This implies fewer multipliers and adders.

For various reasons, a comparison of IIR and FIR filters is more involved that the above remark appears to imply. First, there exist techniques (which are perhaps less readily available), for the design of nonlinear phase FIR filters. For a given magnitude response specification, such FIR filters are less expensive than the linear phase versions. Second, there are some commercial signal processing chips, specifically tailored for the implementation of FIR filters. In these chips, the implementation of IIR filters is not necessarily more efficient. Finally, there exist *multistage* design techniques for the design of narrowband FIR filters (Sec. 4.4) which are sometimes more efficient than IIR filters. It is, therefore, difficult to provide a comparison that is fair under all contexts. In this text, we will merely compare the number of multiplications and additons. It should be cautioned that in many cases these *do not* provide a good measure of complexity.

Working Principle of IIR Filters

An IIR filter has transfer function of the form $H(z) = P(z)/D(z)$, where

$P(z)$ and $D(z)$ are polynomials in z^{-1}. The zeros of $P(z)$ are typically located on the unit circle, and therefore, have the form $e^{j\omega_k}$. They can be seen in the magnitude response plots, since $H(e^{j\omega_k}) = 0$. These zeros are there to provide stopband attenuation. Figure 3.3-1(a) shows a typical plot of the numerator $|P(e^{j\omega})|$ with several zeros on the unit circle.

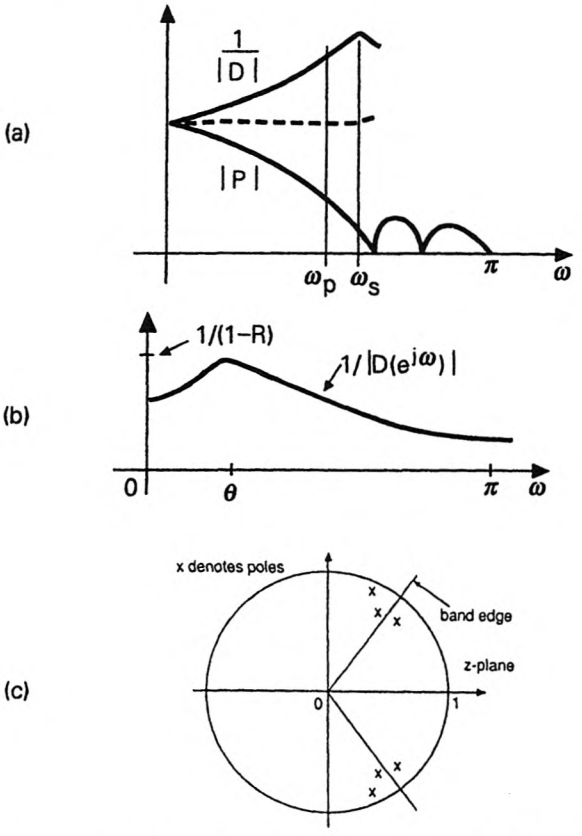

Figure 3.3-1 (a) The roles played by the numerator $P(z)$ and denominator $D(z)$, (b) typical behavior of $1/|D(e^{j\omega})|$ with a single pole, and (c) clustering of poles around the bandedge.

The plot of $|P(e^{j\omega})|$ has the appearance of a lowpass filter, but the passband response is very poor (i.e., not close to unity). The denominator $D(z)$ compensates for this. Figure 3.3-1(a) also indicates a typical response of $1/|D(e^{j\omega})|$, which grows as ω increases in the passband. Thus the magnitude $1/|D(e^{j\omega})|$ is large near the band edge. The product of the two solid curves tends to approximate unity (the broken curve) in the passband.

Figure 3.3-1(b) demonstrates the behavior of $1/|D(e^{j\omega})|$ for the case where $D(z) = 1 - Re^{j\theta}z^{-1}$. Here R and θ are the radius and angle of the pole of $1/D(z)$. We see that the plot has a peak near the pole angle θ. This

peak gets steeper as the pole moves closer to the unit circle (i.e., as $R \to 1$). Since $1/|D(e^{j\omega})|$ is required to have large values near the passband edge, the zeros of $D(z)$ (i.e., poles of the filter) are typically crowded near the band edge [Fig. 3.3-1(c)].

Effect of narrow transition-bands. If the transition bandwidth Δf is small, then the quantity $|P(e^{j\omega_p})|$ gets smaller, so that $1/|D(e^{j\omega_p})|$ has to be 'large' in order for the product to be close to unity. For this reason, the zeros of $D(z)$ are placed *closer* to the unit circle for 'sharp cutoff' filters. Summarizing, the poles are typically crowded near the band edge, and for sharp cutoff filters they are also close to the unit circle.

3.3.1 The Bilinear Transformation

The most common technique to design an IIR filter is to first design an analog filter $H_a(s)$ and convert it into a digital filter using a transformation. Suppose we are given an analog filter with rational transfer function $H_a(s)$, having magnitude response $|H_a(j\Omega)|$ as shown in Fig. 3.3-2. This is lowpass with band edges Ω_p and Ω_S, peak passband ripple δ_1 and peak stopband ripple δ_2. (The frequency ∞ is shown at a finite point just for convenience.) Suppose we take the transfer function and replace the Laplace transform variable s as follows:

$$s = \frac{1 - z^{-1}}{1 + z^{-1}} \quad \text{(bilinear transformation)}. \tag{3.3.1}$$

The result is a rational function $H(z)$ in the variable z^{-1}. With $s = j\Omega$ and $z = e^{j\omega}$, we have from (3.3.1)

$$\Omega = \tan(\omega/2), \tag{3.3.2}$$

which shows that the mapping transforms $\Omega = 0$ into $\omega = 0$, and $\Omega = \infty$ into $\omega = \pi$ (Fig. 3.3-3). The above mapping is called the *bilinear transform* and is the most popular technique to convert analog filters into digital. It can be shown that the transformed version $H(z)$ is stable if and only if $H_a(s)$ is stable.

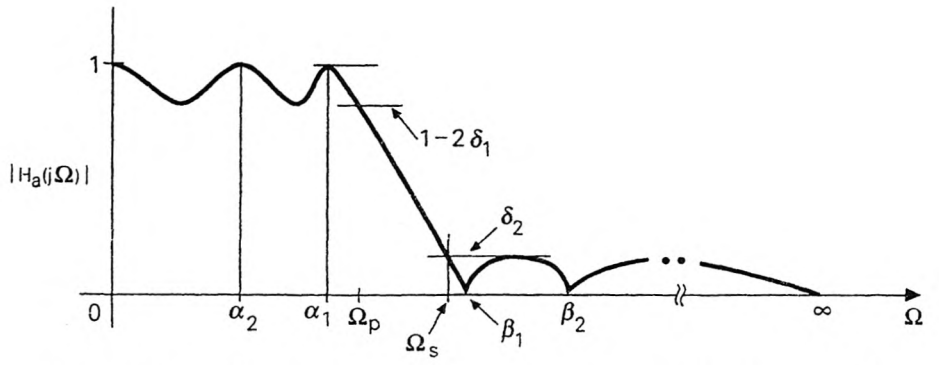

Figure 3.3-2 A typical magnitude response of an analog lowpass filter.

The digital filter response $|H(e^{j\omega})|$ corresponding to the analog response of Fig. 3.3-2 has the appearance shown earlier in Fig. 3.1-1(b). The band-edges ω_p and ω_S are determined by (3.3.2) as

$$\omega_p = 2\arctan\Omega_p, \quad \omega_S = 2\arctan\Omega_S. \tag{3.3.3}$$

The sizes of the ripples δ_1 and δ_2 are unchanged.

If we are given the digital filter specifications $\omega_p, \omega_S, \delta_1$, and δ_2, a design procedure based on bilinear transformation would run as follows: (a) find $\Omega_p = \tan(\omega_p/2)$ and $\Omega_S = \tan(\omega_S/2)$, (b) design the analog filter which meets the specifications $\Omega_p, \Omega_S, \delta_1$, and δ_2, and (c) transform $H_a(s)$ into $H(z)$ using bilinear transformation. It remains only to provide details for the second step, that is, the design of classical analog filters.

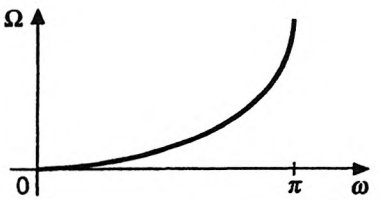

Figure 3.3-3 The frequency mapping property of bilinear transformation.

3.3.2 Analog Filters

The magnitude response for most of the standard analog filters takes the form

$$|H_a(j\Omega)|^2 = \frac{1}{1+F^2(\Omega)} \tag{3.3.4}$$

where $F(\Omega)$ is a real-valued rational function of Ω. Clearly $|H_a(j\Omega)| \leq 1$. The extreme values of the response are

$$|H_a(j\Omega)| = \begin{cases} 1 & \text{if } F(\Omega) = 0 \\ 0 & \text{if } F(\Omega) = \infty. \end{cases} \tag{3.3.5}$$

Butterworth (or Maximally Flat) Filters

The simplest and most illuminating example is the Butterworth filter for which $F(\Omega) = (\Omega/\Omega_c)^N$. So, the frequency response has the form

$$|H_a(j\Omega)|^2 = \frac{1}{1+(\Omega/\Omega_c)^{2N}}. \tag{3.3.6}$$

This is monotone lowpass, and varies from unity (at $\Omega = 0$) to zero (at $\Omega = \infty$). See Fig. 3.3-4. The quantity N is the order of $H_a(s)$. Here is a summary of the main features:

1. We have $|H_a(j\Omega_c)|^2 = 1/2$ which corresponds to an attenuation of 3 dB. So Ω_c is called the *three dB point.* This is not necessarily the passband or stopband edge.
2. For $\Omega >> \Omega_c$ we have

$$-20\log_{10}|H_a(j\Omega)| \approx 20N\log_{10}\Omega - 20N\log_{10}\Omega_c. \tag{3.3.7}$$

This shows that as Ω is increased by one decade (i.e., by a factor of ten) the attenuation increases by $20N$ dB. This is called the $20N$ *dB/decade property* (equivalent to $6.02N$ dB/octave).

3. The first $2N-1$ derivatives of $|H_a(j\Omega)|^2$ are equal to zero at $\Omega = 0$ (see Problem 3.11). This is the maximum possible number of derivatives that can be zero, since $H_a(j\Omega)$ has order N. So, the Butterworth filter is said to be *maximally* flat at $\Omega = 0$.

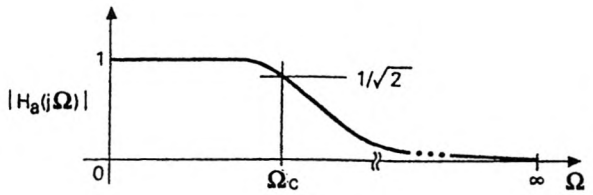

Figure 3.3-4 The magnitude response characteristics of a Butterworth filter.

Expression for the digital transfer function. Since the response is zero only at $\Omega = \pm\infty$, the transfer function $H_a(s)$ has the form

$$H_a(s) = \frac{1}{D_a(s)}, \tag{3.3.8}$$

where

$$D_a(s) = 1 + d_1 s + \ldots + d_N s^N. \tag{3.3.9}$$

(assuming $H_a(0) = 1$.) In other words, $H_a(s)$ is an all-pole filter. After bilinear transformation, the digital Butterworth filter therefore has the form

$$H(z) = \frac{c(1+z^{-1})^N}{B(z)}. \tag{3.3.10}$$

All zeros are now at $z = -1$, that is, at $\omega = \pi$ which corresponds to $\Omega = \infty$. Note that $H(z)$ can be implemented with $2N$ adders and only $N+1$ multipliers (rather than $2N+1$) because of the special form of the numerator.

Location of poles. The N zeros of $D_a(s)$ [poles of the Butterworth filter $H_a(s)$] lie on a circle in the s plane, with center at the origin and radius Ω_c. The pole angles are given by

$$\frac{\pi}{2} + \frac{\pi}{2N} + \frac{k\pi}{N}, \quad 0 \le k \le N-1. \tag{3.3.11}$$

Given Ω_c and N, one can compute the pole locations as above, and hence the coefficients of $D_a(s)$. The pole locations are demonstrated in Fig. 3.3-5 for $N = 3$. The pole angles are $\pm 2\pi/3$ and π so that, with $\Omega_c = 1$, we have

$$\begin{aligned} D_a(s) &= (s+1)(s - e^{j2\pi/3})(s - e^{-j2\pi/3}) \\ &= (s+1)(s^2 + s + 1) = s^3 + 2s^2 + 2s + 1. \end{aligned} \tag{3.3.12}$$

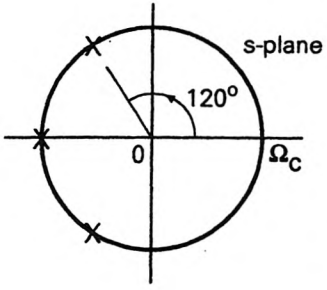

Figure 3.3-5 Pole locations of a third order Butterworth filter.

So, the third order Butterworth lowpass filter with $\Omega_c = 1$ is given by $H_a(s) = 1/(s^3 + 2s^2 + 2s + 1)$.

Note that the transfer function is determined completely by the two parameters N and Ω_c. We have only two degrees of freedom available. In the above example, we see that $D_a(s)$ is a symmetric polynomial; this is true for any N as long as $\Omega_c = 1$.

From the above demonstration, and more generally from (3.3.11) one can see that the poles are in the open left half plane (i.e, $\mathrm{Re}[s] < 0$) so that the filter $H_a(s)$ is always stable.

Design Example 3.3.1: Butterworth Filters

Suppose we wish to design a Butterworth filter with $\Omega_p = 2\pi \times (10\text{kHz})$, $\Omega_S = 2\pi \times (20\text{kHz})$, $A_S = 60$ dB and $A_{max} = 0.1$ dB. This is illustrated in Fig. 3.3-6. Since $A_S = -10\log_{10}|H_a(j\Omega_S)|^2$ and so on, we obtain

$$\begin{aligned} (\Omega_p/\Omega_c)^{2N} &= 10^{A_{max}/10} - 1, \\ (\Omega_S/\Omega_c)^{2N} &= 10^{A_S/10} - 1. \end{aligned} \tag{3.3.13}$$

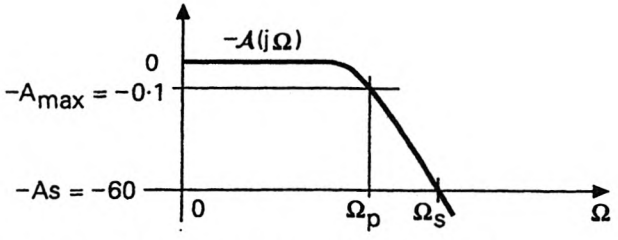

Figure 3.3-6 Specifications in dB for the Butterworth example.

Dividing one equation by the other we eliminate Ω_c and obtain $N = 12.677$. This is the estimated order which should be rounded to the nearest integer, that is, $N = 13$. Since Ω_p, Ω_S, A_S and A_{max} are known we can solve for Ω_c from either equation in (3.3.13). Suppose we use the second equation, then $\Omega_c = \Omega_S/1.701$. The resulting filter has the specified A_S, and the value of A_{max} is slightly better than specified (because N was rounded *up*).

Equiripple Filters

As in the digital FIR case, an analog filter with equiripple response requires smaller order for the same set of ripple sizes and transition bandwidth. A Chebyshev filter, for example, has an equiripple passband. This is obtained by choosing $F(\Omega) = \epsilon C_N(\Omega/\Omega_p)$ in (3.3.4) where $C_N(x)$ is the so-called Nth order Chebyshev polynomial. The transfer function $H_a(s)$ corresponding to this is again all-pole. The filter is optimal in the sense that among all all-pole filters of order N, this filter has the smallest A_{max} for fixed Ω_p, Ω_S, and A_S. We will not discuss Chebyshev filters (or *inverse* Chebyshev filters) further in this text. (However, Problems 3.13 and 3.14 cover some details.)

Elliptic filters

An elliptic filter is an improvement over Chebyshev in the sense that both the passband and stopband are equiripple, as in Fig. 3.3-2. From the figure, we see that there are transmission zeros at finite frequencies, so that $H_a(s)$ is not an all-pole filter. The filter is optimal in the sense that among all rational transfer functions of a given order, elliptic filters have the smallest A_{max} for fixed Ω_p, Ω_S, and A_S.

Design of Elliptic Filters

A simple algorithm for the design of analog elliptic filters is presented in pp. 125 to 128 of Antoniou [1979]. The algorithm designs the coefficients of $H_a(s)$ with magnitude response specified as in Fig. 3.3-2. It is assumed that the bandedges are related as

$$\Omega_p \Omega_S = 1. \tag{3.3.14}$$

This is called the *frequency normalization condition.* Given the quantities δ_1, δ_2 (equivalently A_{max}, A_S) and $r \triangleq \Omega_p/\Omega_S$, the algorithm first estimates the required order which will meet these specifications. This estimate may turn out to be a noninteger. The coefficients of $H_a(s)$ with nearest integer N (or next higher integer N, if the user prefers it) are then calculated.

The complete procedure to design a digital elliptic filter is as follows: given the specifications ω_p, ω_S, δ_1 and δ_2, compute

$$\Omega_p = \tan(\omega_p/2), \quad \Omega_S = \tan(\omega_S/2). \tag{3.3.15}$$

If these bandedges do not satisfy (3.3.14) then define

$$\Omega_p' = \alpha\Omega_p, \quad \Omega_S' = \alpha\Omega_S, \tag{3.3.16}$$

where $\alpha = (\Omega_p \Omega_S)^{-0.5} > 0$. This ensures that the frequency normalization $\Omega'_p \Omega'_S = 1$ holds. We can now design the analog elliptic filter $H'_a(s)$ whose specifications are $\Omega'_p, \Omega'_S, A_{max}$ and A_S. If we define $H_a(s) = H'_a(\alpha s)$, then $H_a(s)$ meets the specifications $\Omega_p, \Omega_S, A_{max}$ and A_S. We finally obtain the digital filter as

$$H(z) = H_a(s)\Big|_{s = (1 - z^{-1})/(1 + z^{-1}).} \tag{3.3.17}$$

The filter can then be implemented using the direct form or cascade form structure (or, better still, using the structure to be derived in Section 3.6, which has least complexity).

For odd N the elliptic lowpass digital filter has one real pole, and a zero at $z = -1$. The remaining poles are complex conjugate pairs and so are the zeros. Furthermore all zeros are on the unit circle. Based on these facts we can express the transfer function as

$$H(z) = a_0 \left(\frac{1 + z^{-1}}{1 + bz^{-1}} \right)^{\ell} \prod_{k=1}^{m} \left(\frac{1 - 2\cos\omega_k z^{-1} + z^{-2}}{1 - 2R_k \cos\phi_k z^{-1} + R_k^2 z^{-2}} \right), \tag{3.3.18}$$

where ω_k are the transmission zeros, ϕ_k are the pole angles and R_k the pole radii for the complex conjugate pairs. (See Chap. 2, discussions around eqs. (2.1.18), and (2.1.19).) The order is $N = 2m + \ell$, where $\ell = 0$ or 1 depending on N.

The numerator of the above $H(z)$ is a symmetric polynomial. The direct form as well as cascade form structures can be implemented with a total of $2N$ additions and about $1.5N$ (rather than $2N + 1$) multipliers because of numerator symmetry.

Design Example 3.3.2: Elliptic Filters

Suppose the digital lowpass filter specifications are $\omega_p = 0.15\pi, \omega_S = 0.20\pi$, $\delta_1 = 0.01$ and $\delta_2 = 0.001$. (This δ_2 implies 60dB attenuation.) By using the above procedure in conjunction with the algorithm in Antoniou [1979], the order of the elliptic filter is estimated as $N = 6.56$, which can be rounded to the integer seven. The resulting digital filter $H(z)$ has magnitude response as shown in Fig. 3.3-7(a), and satisfies the stated specifications. The group delay response is shown in Fig. 3.3-7(b). Since this is not constant, the system has a nonlinear phase response. The group delay shows a variation from about 10 samples to 60 samples.

By using (3.2.32) one can verify that a *linear phase* FIR equiripple filter with same specifications requires an order of 101. The 7th order elliptic IIR filter can be implemented with only 7 multiplications (as we will see in Sec. 3.6) whereas the FIR filter requires 51 multipliers!

Comparison with Butterworth filters. Because of the equiripple nature in both passband and stopband, the elliptic filter requires much

smaller order that a Butterworth filter meeting same specifications. In the above design example, a Butterworth filter would require an order of 28.

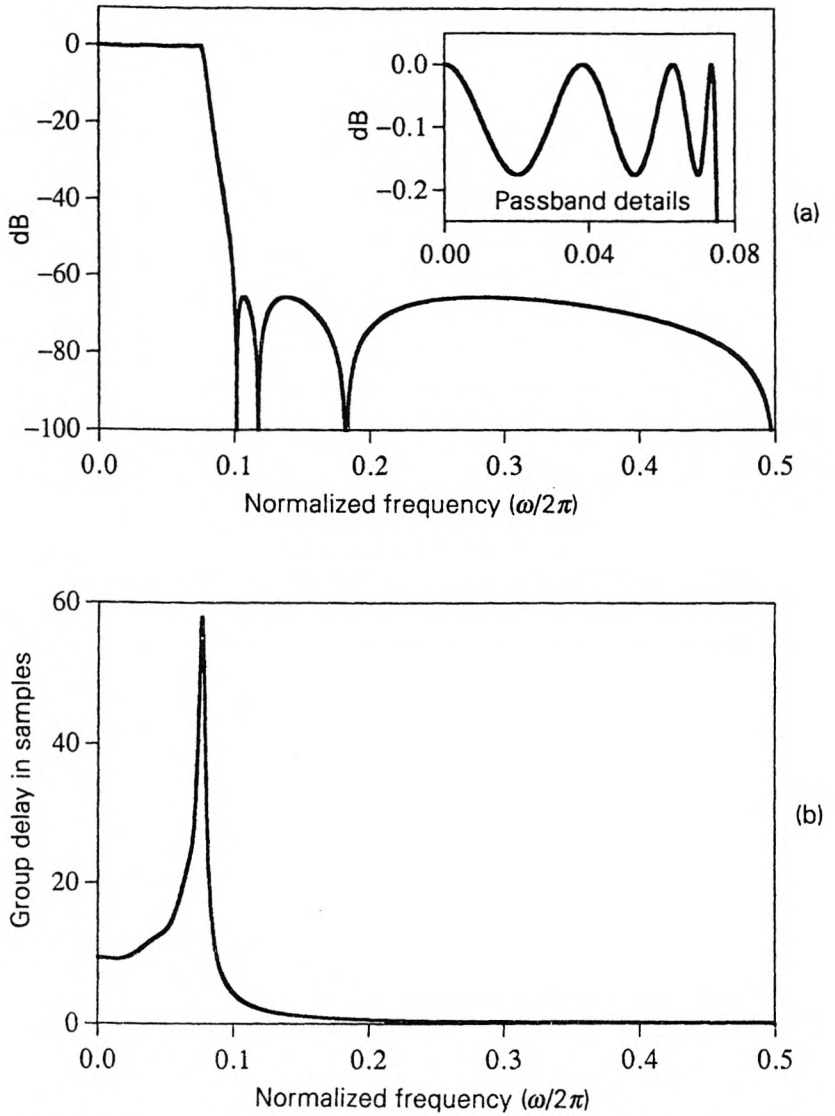

Figure 3.3-7 Design example 3.3.2. Responses of the elliptic filter. (a) Magnitude and (b) group delay.

3.3.3 Properties of Digital Elliptic Filters

Elliptic filters are very important in the design of multirate filter banks, as we will see in Chap. 5. For this reason we now describe their most important features. Since we will be using digital elliptic filters (i.e., bilinearly

transformed analog elliptic filters), our discussions will directly address the digital transfer function $H(z)$.

For any real transfer function, we can write $|H(e^{j\omega})|^2$ as $H(z^{-1})H(z)$ (with $z = e^{j\omega}$). This is notationally more convenient. For an elliptic filter, $H(z^{-1})H(z)$ takes the form

$$H(z^{-1})H(z) = \frac{1}{1 + \epsilon^2 R(z)R(z^{-1})}, \tag{3.3.19}$$

where $R(z)$ is a rational function of the form

$$R(z) = \left(\frac{1 - z^{-1}}{1 + z^{-1}}\right)^{\ell} \prod_{k=1}^{m} \frac{(1 - z^{-1}e^{j\theta_k})(1 - z^{-1}e^{-j\theta_k})}{(1 - z^{-1}e^{j\omega_k})(1 - z^{-1}e^{-j\omega_k})}. \tag{3.3.20}$$

The order of $H(z)$ is given by $N = 2m + \ell$, with

$$\ell = \begin{cases} 1 & N \text{ odd} \\ 0 & N \text{ even.} \end{cases} \tag{3.3.21}$$

If we set $z = e^{j\omega}$ then $R(z)R(z^{-1}) = |R(e^{j\omega})|^2 \geq 0$ so that

$$|H(e^{j\omega})|^2 = \frac{1}{1 + \epsilon^2 |R(e^{j\omega})|^2} \leq 1. \tag{3.3.22}$$

It is easily verified that

$$|H(e^{j\omega})|^2 = \begin{cases} 0 & \text{for } \omega = \omega_k, \\ 1 & \text{for } \omega = \theta_k. \end{cases} \tag{3.3.23}$$

This is illustrated in Fig. 3.3-8 for $N = 5$ and $N = 6$. There are precisely N frequencies (in the region $0 \leq \omega < 2\pi$) where $|H(e^{j\omega})| = 1$, and N frequencies where $|H(e^{j\omega})| = 0$. For odd N we have $\ell = 1$ so that $|H(e^{j0})| = 1$ and $|H(e^{j\pi})| = 0$. For even N this is not true. By inspecting plots of the form in Fig. 3.3-8 one can immediately identify the order of the elliptic filter.

The frequencies ω_k, as we know, are the transmission zeros of $H(z)$. The frequencies θ_k, where $|H(e^{j\omega})| = 1$ (maximum magnitude) are called the reflection zeros.† The values of θ_k and ω_k are such that the response $|H(e^{j\omega})|$ has equiripple behavior.

The elliptic family. It turns out that for a given ω_p, ω_S, and N, the quantities θ_k and ω_k are fixed. The parameter ϵ in (3.3.19) acts as a tradeoff

† This name has to do with doubly terminated LC realizations of electrical filters; the interested reader can see Chap. 12 in Antoniou [1979].

between δ_1 and δ_2 (Fig. 3.3-9). By varying ϵ, one spans a complete family of elliptic transfer functions. Each ϵ corresponds to a unique elliptic filter in the family.

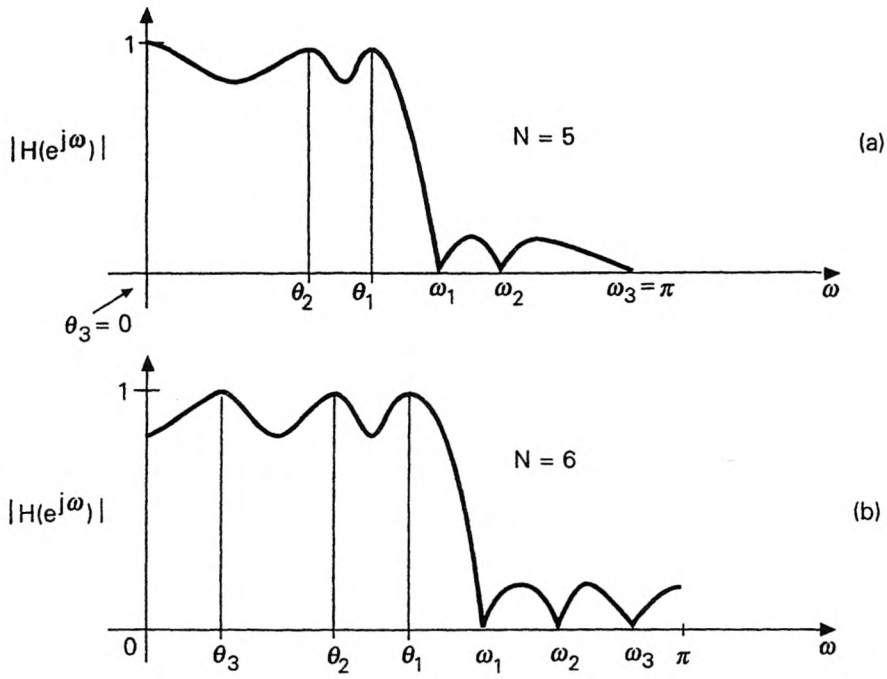

Figure 3.3-8 Typical responses of digital elliptic lowpass filters (a) odd order ($N = 5$), and (b) even order ($N = 6$).

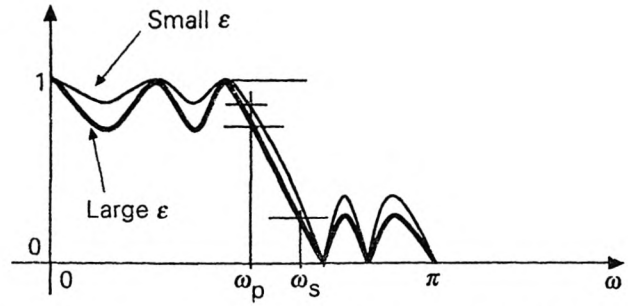

Figure 3.3-9 Two responses belonging to the same elliptic family characterized by w_p, w_S and N. The two curves differ only in terms of ϵ.

Uniqueness. Suppose $G(z)$ is an Nth order stable equiripple lowpass filter with bandedges ω_p, ω_S and the same number of ripples as an Nth order

elliptic lowpass filter. Then, $G(z)$ is elliptic and belongs to the elliptic family characterized by N, ω_p, and ω_S.

3.4 ALLPASS FILTERS

Allpass filters play an important role in some multirate applications. Prominent among these is the two channel IIR QMF bank to be discussed in Sec. 5.3. In this section we study the fundamental properties of allpass functions. A tutorial on allpass filters can be found in Regalia, et al. [1988].

Definition and examples. A discrete-time transfer function $H(z)$ is said to be allpass if

$$|H(e^{j\omega})| = c, \quad c > 0, \qquad \text{for all } \omega, \tag{3.4.1}$$

that is, the magnitude response is constant. As a result the frequency response has the form

$$H(e^{j\omega}) = ce^{j\phi(\omega)}, \tag{3.4.2}$$

where $\phi(\omega)$ is the phase response. If $|H(e^{j\omega})| = 1$ (i.e., $|c| = 1$) we say that $H(z)$ is unit-magnitude allpass.

Simple examples of allpass functions are: $H(z) = 1$ and $H(z) = z^{-K}$ where K is an integer. A nontrivial example is the first-order filter

$$H(z) = \frac{a^* + z^{-1}}{1 + az^{-1}}. \tag{3.4.3}$$

To verify that this is allpass, rewrite

$$H(z) = z^{-1}\frac{1 + a^*z}{1 + az^{-1}} \tag{3.4.4}$$

so that the frequency response is

$$H(e^{j\omega}) = e^{-j\omega}\left(\frac{1 + a^*e^{j\omega}}{1 + ae^{-j\omega}}\right). \tag{3.4.5}$$

Clearly, $|H(e^{j\omega})| = 1$ for all ω.

More complicated examples can be obtained by multiplying first order filters of the form (3.4.3) because the product of two allpass functions is allpass. The sum of two allpass functions is, in general, not allpass. For example $H_1(z) = 1$ and $H_2(z) = z^{-1}$ are allpass but their sum has magnitude response $2\cos(\omega/2)$ which is not constant.

3.4.1 Properties of Allpass Functions

We restrict attention only to allpass functions which can be expressed as rational functions (though not necessarily with real coefficients). In what

follows, we will freely use notations and terms such as "tilde", "dagger", subscript asterik, and "generalized-Hermitian", which are summarized in Sec. 2.3.

It is often convenient to express the property (3.4.1) in terms of the z-transform variable. For this note that (3.4.1) is equivalent to the property

$$\widetilde{H}(z)H(z) = c^2, \quad z = e^{j\omega}. \tag{3.4.6}$$

Invoking analytic continuation (Sec. 2.4.3), we see that this implies

$$\widetilde{H}(z)H(z) = c^2, \quad \text{for all } z. \tag{3.4.7}$$

We can verify this for (3.4.3) as follows:

$$\widetilde{H}(z)H(z) = \left(\frac{a+z}{1+a^*z}\right)\left(\frac{a^*+z^{-1}}{1+az^{-1}}\right) = \left(\frac{1+az^{-1}}{a^*+z^{-1}}\right)\left(\frac{a^*+z^{-1}}{1+az^{-1}}\right) = 1. \tag{3.4.8}$$

The allpass property, expressed in the form (3.4.7), will be frequently used to derive deeper properties.

A. Poles and Zeros of Allpass Functions

The poles and zeros of an allpass function occur in *reciprocal conjugate* pairs. In other words, if α is a pole, then its reciprocal conjugate $1/\alpha^*$ is a zero. This is easily verified for (3.4.3), where the pole $= -a$ and the zero $= -1/a^*$ indeed.

For a general proof, note that (3.4.7) yields

$$\widetilde{H}(\alpha) = \frac{c^2}{H(\alpha)} = \frac{c^2}{\infty} = 0 \quad (\text{since } H(\alpha) = \infty). \tag{3.4.9}$$

In view of the definition of the 'tilde' notation this implies

$$H_*(1/\alpha) = 0. \tag{3.4.10}$$

Conjugating both sides and exploiting the meaning of "subscript asterik" we see that this in turn implies $H(1/\alpha^*) = 0$. That is, $1/\alpha^*$ is a zero of $H(z)$.

B. Most General Form of Rational Allpass Functions

Suppose $H_N(z)$ is an Nth order rational allpass function with a pole at α_1. This implies that $H_N(z)$ has a zero at $1/\alpha_1^*$ so that $H_N(z)$ has the factor $(-\alpha_1^* + z^{-1})/(1 - \alpha_1 z^{-1})$. This factor is clearly a first order allpass function. We can then write

$$H_N(z) = \left(\frac{-\alpha_1^* + z^{-1}}{1 - \alpha_1 z^{-1}}\right) H_{N-1}(z). \tag{3.4.11}$$

By taking magnitudes on both sides, we see that $H_{N-1}(z)$ is allpass (with order $N-1$). Repeating the above factorization process, we arrive at

$$H_N(z) = \beta \prod_{k=1}^{N} \frac{-\alpha_k^* + z^{-1}}{1 - \alpha_k z^{-1}}, \quad \beta \neq 0, \tag{3.4.12}$$

where β is a (possibly complex) constant. Summarizing, we have proved that an Nth order allpass function has the general form (3.4.12). Note that if $\alpha_k = 0$ for some k, the corresponding factor reduces to z^{-1}. Thus, the special case $H_N(z) = \beta z^{-N}$ is also covered by the above form.

Most general unfactored form: The form (3.4.12) is induced by the fact that the poles and zeros of an allpass function come in reciprocal conjugate pairs. It is often convenient to write an expression for an allpass function in unfactored form. This can be done by multiplying out the factors in (3.4.12). It can be shown that after such multiplication the result takes the form

$$H(z) = d\frac{b_N^* + b_{N-1}^* z^{-1} + \ \ldots\ + b_1^* z^{-(N-1)} + b_0^* z^{-N}}{b_0 + b_1 z^{-1} + \ \ldots\ + b_N z^{-N}}, \quad d > 0. \tag{3.4.13}$$

We have restricted d to be real and positive because b_0 can be arbitrary.

Except for the scale factor d, the numerator coefficients are therefore obtainable by writing the denominator coefficients in reverse order and conjugating them. In other words if $H(z) = A(z)/B(z)$ with

$$A(z) = \sum_{n=0}^{N} a_n z^{-n}, \quad B(z) = \sum_{n=0}^{N} b_n z^{-n}, \tag{3.4.14}$$

then $a_n = db_{N-n}^*$. We can express this in the z-domain as

$$A(z) = dz^{-N}\widetilde{B}(z), \tag{3.4.15}$$

so that (3.4.13) reduces to the form

$$H(z) = dz^{-N}\frac{\widetilde{B}(z)}{B(z)}. \tag{3.4.16}$$

So any rational allpass filter can be expressed as above.

Conversely, the form (3.4.12) is allpass since each factor is allpass. Similarly any transfer function of the form (3.4.16) is allpass because

$$H(e^{j\omega}) = de^{-j\omega N}\frac{B^*(e^{j\omega})}{B(e^{j\omega})}, \tag{3.4.17}$$

which has magnitude d for all ω.

Summarizing, an Nth order rational function $H(z)$ is allpass if and only if it can be expressed as in (3.4.16) for $d > 0$ [or equivalently as in (3.4.12)]. Furthermore, for unit-magnitude allpass functions, we can always take $d = 1$.

C. Energy Balance Property (Losslessness)

Let $u(n)$ and $y(n)$ be the input and output of a stable allpass filter $H(z)$. In view of (3.4.1) we have $|Y(e^{j\omega})| = c|U(e^{j\omega})|$. So,

$$\int_0^{2\pi} |Y(e^{j\omega})|^2 \frac{d\omega}{2\pi} = c^2 \int_0^{2\pi} |U(e^{j\omega})|^2 \frac{d\omega}{2\pi}, \tag{3.4.18}$$

for any input $u(n)$. By Parseval's theorem this implies

$$\underbrace{\sum_{n=-\infty}^{\infty} |y(n)|^2}_{\text{output energy } E_y} = c^2 \underbrace{\sum_{n=-\infty}^{\infty} |u(n)|^2}_{\text{input energy } E_u} . \tag{3.4.19}$$

Thus $E_y = c^2 E_u$, that is, the energy-amplification factor c^2 is independent of the input. In particular if $c = 1$ in (3.4.1), then the output energy is equal to the input energy for all possible input sequences. For this reason allpass functions are also called *lossless functions*, (whether $c = 1$ or not).

D. Time Domain Meaning of Allpass Property

In Problem 2.14, we defined the autocorrelation $r(k)$ of a sequence $h(n)$ to be

$$r(k) = \sum_{n=-\infty}^{\infty} h(n)h^*(n-k).$$

From this problem we can conclude that the z-transform of $r(k)$ is given by $R(z) = \widetilde{H}(z)H(z)$. If $H(z)$ is allpass, $\widetilde{H}(z)H(z) = c^2$. This implies that $r(k)$ is an unit pulse function, that is,

$$r(k) = c^2\delta(k). \tag{3.4.20}$$

Conversely, if $r(k)$ is an unit pulse, then its z-transform $\widetilde{H}(z)H(z)$ is constant and $H(z)$ is allpass. Summarizing, $H(z)$ is allpass if and only if the autocorrelation of $h(n)$ is a unit pulse.

E. The Modulus Property of Allpass Functions

We now derive a property of causal stable allpass functions based on a well-known theorem in the theory of complex variables [Churchill and Brown, 1984] called the maximum modulus theorem. This property was observed in [Schüssler, 1976].

♠**The maximum modulus theorem.** Let $F(z)$ be a complex function of the complex variable z. Let $F(z)$ be analytic on and inside a closed contour C in the z-plane (Fig. 3.4-1). Let the maximum value of $|F(z)|$ on the contour C be denoted F_{max}. Then we have $|F(z)| \leq F_{max}$ for all z inside the contour C. Equality holds somewhere inside the contour *if and only if* $F(z)$ *is constant.* ◊

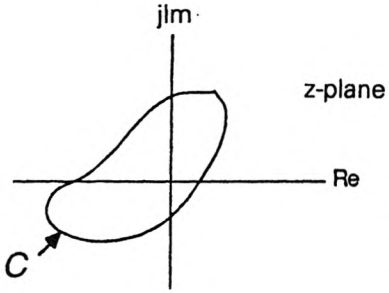

Figure 3.4-1 Pertaining to the maximum modulus theorem.

Now let $H(z)$ be a transfer function with all poles strictly inside the unit circle of the z-plane. Let $|H(e^{j\omega})|$ have maximum value (that is, maximum over all ω) equal to c. By defining $F(z) = H(1/z)$ and invoking the maximum modulus theorem we conclude that $|H(z)| \leq c$ for all z *outside* the unit circle. Equality holds for some z outside the unit circle if and only if $H(z)$ is a constant.

In particular, if the above $H(z)$ is allpass, then more is true. In this case we can also make a claim about the magnitude $|H(z)|$ *inside* the unit circle. For this note that (3.4.7) implies

$$\widetilde{H}(\alpha) = \frac{c^2}{H(\alpha)} \tag{3.4.21}$$

for any α. Using the fact that $\widetilde{H}(\alpha) = H_*(1/\alpha)$ and conjugating both sides,

$$H(1/\alpha^*) = \frac{c^2}{H^*(\alpha)}. \tag{3.4.22}$$

For $|\alpha| > 1$ we know $|H(\alpha)| < c$ so that by taking magnitudes we get

$$|H(1/\alpha^*)| > c \tag{3.4.23}$$

for every α outside the unit circle, that is, $|H(\beta)| > c$ for every β inside the unit circle.

Summarizing we have proved this: if $H(z)$ is a causal stable allpass function with $|H(e^{j\omega})| = c$, then

$$|H(z)| \begin{cases} < c, & \text{for } |z| > 1 \\ > c, & \text{for } |z| < 1 \\ = c, & \text{for } |z| = 1, \end{cases} \tag{3.4.24}$$

unless $H(z)$ is constant for all z. The example $H(z) = z^{-1}$ provides a simple way to remember the above inequalities.

F. The Monotone Phase-Response Property

Consider the delay function $H(z) = z^{-K}, K > 0$. This is allpass with $H(e^{j\omega}) = e^{-j\omega K}$. The phase response is $\phi(\omega) = -K\omega$, which is a monotone decreasing function spanning a total range of $2\pi K$ as ω increases from 0 to 2π. More generally, let $H(z)$ be any rational Nth order allpass function. If $H(z)$ has all poles inside the unit circle, we will prove that $\phi(\omega)$ is monotone decreasing, and spans a range of $2\pi N$ as ω increases from 0 to 2π.

First order case. First consider $H(z) = (a^* + z^{-1})/(1 + az^{-1})$. The pole is at $z = -a$. Let R and θ represent the radius and angle of the pole so that $a = -Re^{j\theta}$. Then

$$H(e^{j\omega}) = e^{-j\omega} \frac{1 - Re^{j(\omega-\theta)}}{1 - Re^{-j(\omega-\theta)}}. \tag{3.4.25}$$

The phase response $\phi(\omega)$ can be obtained from this as

$$\phi(\omega) = -\omega + 2\tan^{-1} \frac{R\sin(\omega - \theta)}{R\cos(\omega - \theta) - 1}. \tag{3.4.26}$$

Differentiating with respect to ω we arrive at

$$\frac{d\phi(\omega)}{d\omega} = \frac{-(1 - R^2)}{(1 - R)^2 + 2R[1 - \cos(\omega - \theta)]}. \tag{3.4.27}$$

If the pole is inside the unit circle, we have $0 \leq R < 1$. So $d\phi(\omega)/d\omega < 0$, that is, $\phi(\omega)$ is monotone decreasing.

Figure 3.4-2 demonstrates this for $\theta = 0$ (real pole at $-R$). As ω varies from 0 to 2π, the range spanned by the phase is 2π. For arbitrary θ we can simply shift this curve by θ (and add a constant) to obtain $\phi(\omega)$. If the pole is outside the unit circle, then all discussions remain the same except that the phase is monotone *increasing.*

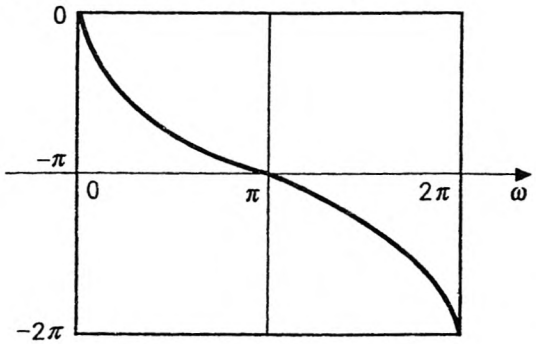

Figure 3.4-2 The monotone phase response of a first order allpass filter ($\theta = 0$).

Since an Nth order stable allpass function is a product of N first order stable allpass functions, its (unwrapped) phase response is the sum of the N individual phase responses, and is thus monotone. The range spanned by $\phi(\omega)$ is the sum of individual ranges, that is, $2\pi N$.

The converse result. Suppose $H(z)$ is a causal Nth order allpass function with monotone decreasing phase response spanning a range of $2\pi N$ as ω varies from 0 to 2π. This is possible only if each of the N first order factors has a monotone decreasing phase response. So, each factor is stable, showing that $H(z)$ is stable.

Some of the above discussions turn out to be conceptually simpler if we think in terms of *continuous time* allpass functions. See Problems 3.17 and 3.18.

3.4.2 Simple Structures for Allpass Filters

Figure 3.4-3 shows the direct form structure for the first order allpass function $H(z) = (a^*+z^{-1})/(1+az^{-1})$. It has one (complex) delay, two (complex) multipliers and two (complex) adders. For the real coefficient case we have $a = a^*$ and the equivalent structure of Fig. 3.4-4 can be obtained (since a and z^{-1} are interchangeable in this case).

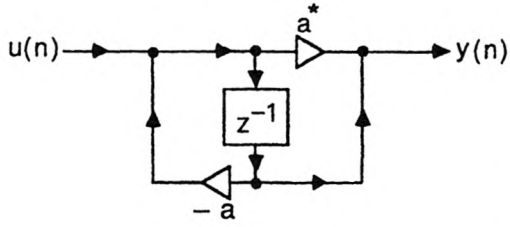

Figure 3.4-3 The direct form structure for a first order allpass function.

An arbitrary Nth order allpass function can be implemented by cascading first order sections (Fig. 3.4-5). For the real-coefficient case we know that poles (and zeros) are either real or occur in complex conjugate pairs so that the allpass function is a product of first order sections of the form

$$H_{1,k}(z) = \frac{a_k + z^{-1}}{1 + a_k z^{-1}}, \quad a_k \text{ real}, \tag{3.4.28}$$

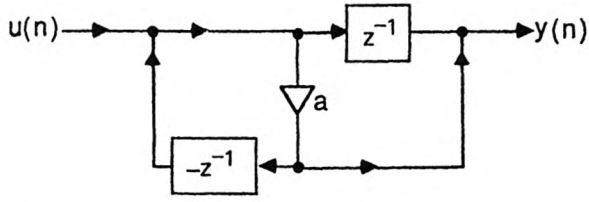

Figure 3.4-4 A one-multiplier implementation of a real coefficient first order allpass function.

second order sections of the form

$$H_{2,k}(z) = \frac{R_k^2 - 2R_k \cos\theta_k z^{-1} + z^{-2}}{1 - 2R_k \cos\theta_k z^{-1} + R_k^2 z^{-2}} \tag{3.4.29}$$

and a scale factor β.

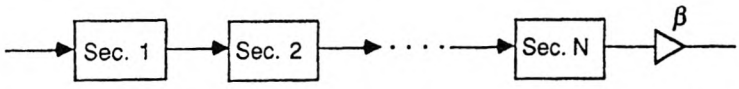

Figure 3.4-5 Cascade form implementation of an Nth order allpass function. Each section is first-order allpass.

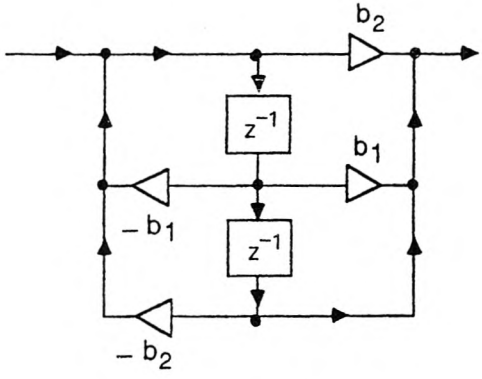

(a) 4 multiplier, 2 delay version

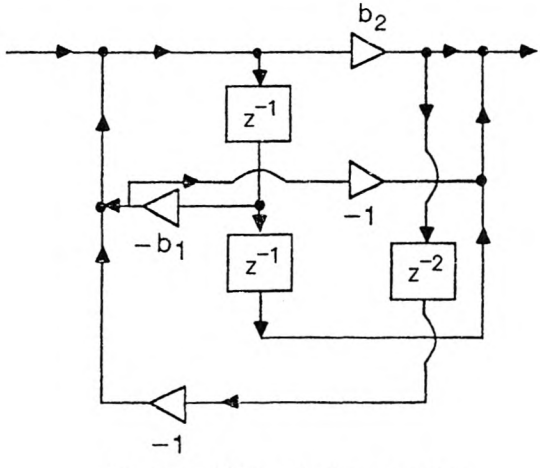

(b) 2 multiplier, 4 delay version

Figure 3.4-6 Direct form structures for second order real coefficient allpass fuctions (a) 4 multiplier, 2 delay version, and (b) 2 multiplier, 4 delay version.

A real-coefficient second order section can be implemented as in Fig. 3.4-6(a) requiring four multipliers, four adders and two delays. A second implementation requiring two multipliers, four adders and four delays is shown in Fig. 3.4-6(b). It is possible to obtain more efficient implementations having the smallest possible number of multipliers and delays. One of these is the one-multiplier lattice structure to be derived in the next section. Several other interesting allpass structures have been derived in Mitra and Hirano [1974], by use of a systematic technique called the multiplier extraction approach. Also see Szczupak, et al. [1988].

3.4.3 Lattice Structures for Allpass Filters

We now derive an allpass structure called the *cascaded lattice structure,* also known as the *Gray and Markel structure* [Gray and Markel, 1973]. Such a structure can be derived for any Nth order stable unit-magnitude allpass filter, and has the property that all multipliers have magnitude less than unity. Its importance lies in the fact that the transfer function remains stable (and allpass) inspite of multiplier quantization, as long as the multiplier magnitudes remain less than unity. The derivation of this structure depends on the following result.

♠**Theorem 3.4.1. The order reduction step.** Let $G_m(z)$ be an mth order causal, stable, unit-magnitude allpass function. Then it can be implemented as in Fig. 3.4-7 where (a) $|k_m| < 1$, and (b) $G_{m-1}(z)$ is a causal, stable, unit-magnitude allpass function with order $m-1$. ◊

Proof. $G_m(z)$ has the form $G_m(z) = z^{-m}\widetilde{B}_m(z)/B_m(z)$ where

$$B_m(z) = b_{m,0} + b_{m,1}z^{-1} + \ldots + b_{m,m}z^{-m}. \tag{3.4.30}$$

$B_m(z)$ has all zeros inside the unit circle, since $G_m(z)$ is stable. Now Fig. 3.4-7 implies

$$G_m(z) = \frac{k_m^* + z^{-1}G_{m-1}(z)}{1 + k_m z^{-1}G_{m-1}(z)}. \tag{3.4.31}$$

Equivalently, by inversion of this, we have

$$z^{-1}G_{m-1}(z) = \frac{G_m(z) - k_m^*}{1 - k_m G_m(z)}, \tag{3.4.32}$$

that is,

$$z^{-1}G_{m-1}(z) = \frac{z^{-m}\widetilde{B}_m(z) - k_m^* B_m(z)}{B_m(z) - k_m z^{-m}\widetilde{B}_m(z)}. \tag{3.4.33}$$

Our aim is to show that there exists k_m with $|k_m| < 1$, such that the right-hand side above does indeed have the form $z^{-1}G_{m-1}(z)$, with $G_{m-1}(z)$ having the stated properties. It is clear that k_m must be such that the polynomial $B_m(z) - k_m z^{-m}\widetilde{B}_m(z)$ has order $m-1$ (so that it can be taken as

the denominator of $G_{m-1}(z)$.) By using the definition of *tilde* we see that this polynomial has highest term

$$(b_{m,m} - k_m b^*_{m,0})z^{-m}, \tag{3.4.34}$$

so that the only possible choice of k_m is

$$k_m = b_{m,m}/b^*_{m,0}. \tag{3.4.35}$$

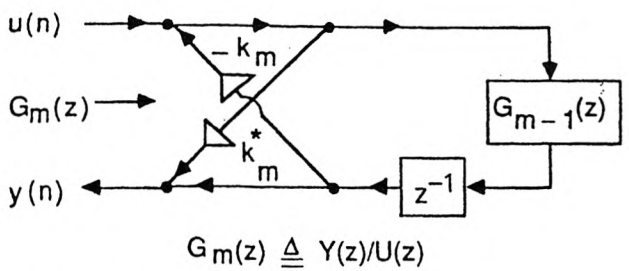

Figure 3.4-7 Generation of an allpass function $G_m(z)$ from a lower order allpass function $G_{m-1}(z)$.

Now the constant term in the numerator polynomial $z^{-m}\widetilde{B}_m(z) - k^*_m B_m(z)$ is $b^*_{m,m} - k^*_m b_{m,0}$ which automatically reduces to zero by the above choice of k_m. As a result, the ratio on the righthand side of (3.4.33) has the form $z^{-1}A_{m-1}(z)/B_{m-1}(z)$, where $A_{m-1}(z)$ and $B_{m-1}(z)$ are polynomials in z^{-1} with order $\leq m-1$. From the relation $z^{-1}A_{m-1}(z) = z^{-m}\widetilde{B}_m(z) - k^*_m B_m(z)$ it is easy to verify that $A_{m-1}(z) = z^{-(m-1)}\widetilde{B}_{m-1}(z)$ so that $G_{m-1}(z) = z^{-(m-1)}\widetilde{B}_{m-1}(z)/B_{m-1}(z)$.

Summarizing, the above choice of k_m ensures that $G_{m-1}(z)$ in (3.4.32) is indeed a causal allpass function, with order $m-1$. [It cannot be less than $m-1$, as $G_m(z)$ in (3.4.31) has order m.] To prove that $|k_m| < 1$, note that the magnitude of the product of all roots of $B_m(z)$ is equal to $|b_{m,m}/b_{m,0}|$. Since all poles of $G_m(z)$ are inside the unit circle, this implies $|k_m| < 1$ indeed.

Next, let α be a pole of $G_{m-1}(z)$. From (3.4.32) we then have $1 - k_m G_m(\alpha) = 0$ so that $|G_m(\alpha)| = 1/|k_m| > 1$. In view of the modulus property (3.4.24), this implies $|\alpha| < 1$ proving that all poles of $G_{m-1}(z)$ are inside the unit circle, that is, $G_{m-1}(z)$ is stable. $\triangledown\triangledown\triangledown$

Repeated Application of the Order Reduction Step

We can repeat the order reduction step, and express $G_{m-1}(z)$ in terms of a reduced order allpass function $G_{m-2}(z)$. If we continue this we finally obtain the constant function G_0 with $|G_0| = 1$. This proves that an Nth order unit-magnitude allpass function $G_N(z)$ with all poles inside the unit

circle can be implemented with the cascaded lattice structure of Fig. 3.4-8, with $|k_m| < 1$ for all m. The N quantities k_m are called the *lattice coefficients* of $G_N(z)$. All multipliers (k_m and k_m^*) in the structure have magnitude less than unity.

The real-coefficient case. If $G_N(z)$ has real coefficients, then k_N is real [see (3.4.35)], so that $G_{N-1}(z)$ also has real coefficients. So all the lattice coefficients k_m are real. Since G_0 has the form $\widetilde{B}_0/B_0$, we have $G_0 = 1$.

The Lattice Guarantees Stability and Allpass Property

We saw above that any causal, stable, unit magnitude allpass function $G_N(z)$ can be implemented as in Fig. 3.4-8, where $|k_m| < 1$ and $|G_0| = 1$. Conversely, the transfer functions $G_m(z)$ indicated in the figure are stable unit-magnitude allpass filters, as long as $|k_m| < 1$ and $|G_0| = 1$. This can be proved by a minor variation of the above reasonings (Problem 3.19). One consequence of this property is that, stability and allpass property are preserved inspite of quantization of k_m, as long as the quantized multipliers satisfy $|k_m| < 1$ and $|G_0| = 1$.

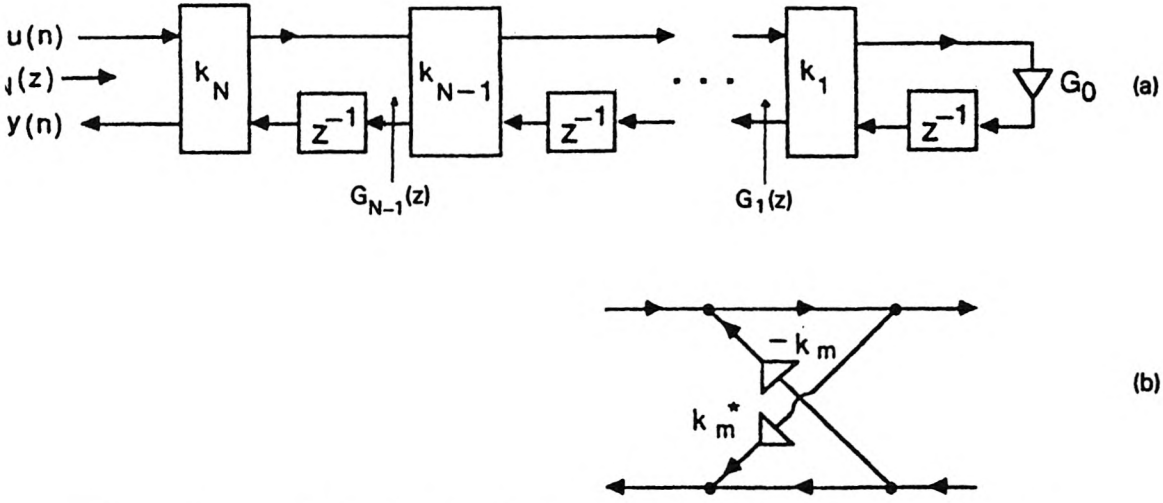

Figure 3.4-8 (a) The cascaded lattice structure, and (b) details of the rectangular boxes labelled k_m.

Variations of the Lattice Structure

Many variations of the lattice structure are known. We now present two of these, which are particularly attractive in practice. To derive these, notice that the structure of Fig. 3.4-7 can be schematically represented as

in Fig. 3.4-9, where the quantities $T_{ij}(z)$ are

$$T_{00}(z) = k_m^*,\ T_{01}(z) = (1 - |k_m|^2)z^{-1},\ T_{10}(z) = 1,\ T_{11}(z) = -k_m z^{-1}. \tag{3.4.36}$$

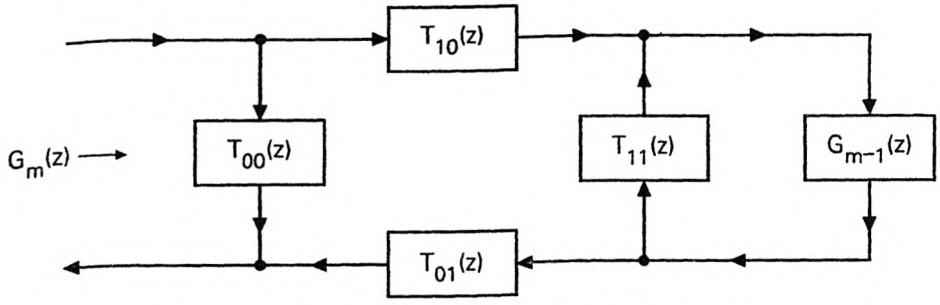

Figure 3.4-9 Schematic redrawing of Fig. 3.4-7.

More generally, for arbitrary $T_{ij}(z)$, the relation between $G_m(z)$ and $G_{m-1}(z)$ is given by

$$G_m(z) = T_{00}(z) + \frac{T_{01}(z)T_{10}(z)G_{m-1}(z)}{1 - T_{11}(z)G_{m-1}(z)}. \tag{3.4.37}$$

Thus, $G_m(z)$ is unchanged if we change $T_{01}(z)$ and $T_{10}(z)$ in such a way that the product $T_{10}(z)T_{01}(z)$ is unchanged. For example if

$$T_{00}(z) = k_m^*,\ T_{01}(z) = \hat{k}_m z^{-1},\ T_{10}(z) = \hat{k}_m,\ T_{11}(z) = -k_m z^{-1}, \tag{3.4.38}$$

where

$$\hat{k}_m = \sqrt{1 - |k_m|^2}, \tag{3.4.39}$$

then $G_m(z)$ is unchanged, for a given $G_{m-1}(z)$. The resulting lattice section, shown in Fig. 3.4-10, is called the *normalized lattice*. An advantage of this structure is that the internal signals are automatically scaled in a certain sense [Gray and Markel, 1975].

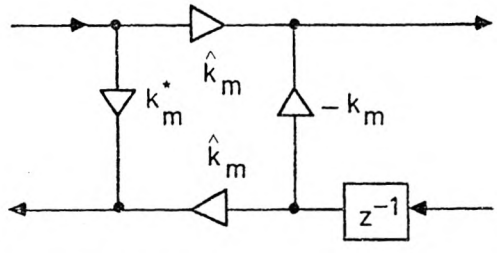

Figure 3.4-10 The normalized lattice section.

For the special case of real coefficient filters, the choice

$$T_{00}(z) = k_m,\ T_{01}(z) = (1 + k_m)z^{-1},\ T_{10}(z) = (1 - k_m),\ T_{11}(z) = -k_m z^{-1}, \tag{3.4.40}$$

results in a useful structure, requiring only one multiplier per lattice section! This structure is shown in Fig. 3.4-11, and requires an extra adder. The complete allpass lattice structure, therefore, requires N real multipliers, N delays and $3N$ adders.

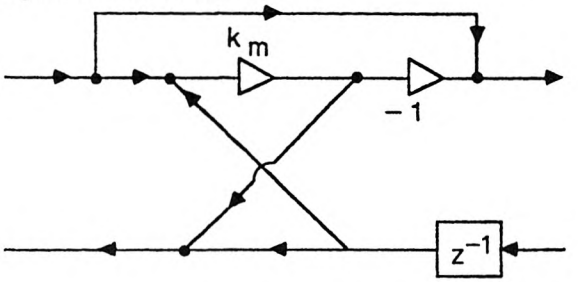

Figure 3.4-11 The one-multiplier lattice section for real coefficient allpass filters.

3.5 SPECIAL TYPES OF FILTERS

We now summarize a number of special transfer functions, that arise frequently in this text.

1. Linear phase transfer functions (Sec. 2.4.2).
2. Allpass transfer functions (Sec. 3.4).
3. *Bounded and BR transfer functions.* If $H(z)$ is stable and such that $|H(e^{j\omega})| \leq 1$, then we say that $H(z)$ is bounded. A bounded transfer function with real coefficients is said to be bounded real (BR).
4. *Lossless transfer functions.* A transfer function is said to be lossless if it is stable and allpass. The name arises from the fact that for such a system the input and output energies are related as $E_y = c^2 E_u$, for all finite-energy inputs. (If $c^2 = 1$, the name "lossless" is particularly appealing, but this condition is not there in the definition.)
5. *LBR transfer functions.* A lossless transfer function with real coefficients is said to be (LBR). So an LBR function is a real-coefficient stable allpass function.
6. *Power complementary transfer functions.* Two transfer functions $H_0(z)$ and $H_1(z)$ are said to be power complementary if

$$|H_0(e^{j\omega})|^2 + |H_1(e^{j\omega})|^2 = c^2 > 0, \quad \text{for all } \omega. \tag{3.5.1a}$$

This can also be rewritten as

$$\tilde{H}_0(z)H_0(z) + \tilde{H}_1(z)H_1(z) = c^2 > 0, \tag{3.5.1b}$$

with $z = e^{j\omega}$. Since our filters are always rational functions, this condition holds *for all* z (Sec. 2.4.3). In practice the transfer functions are scaled so that $c^2 = 1$. Thus, if $H_0(z)$ is a good lowpass filter, then $H_1(z)$ is a good highpass filter. As a generalization, a set of M transfer functions $H_k(z)$ is said to be power complementary if

$$\sum_{k=0}^{M-1} |H_k(e^{j\omega})|^2 = c^2 > 0, \quad \text{for all } \omega. \tag{3.5.2}$$

This concept will be used in many chapters.

7. *Mth band or Nyquist(M) filters.* These will be described in Section 4.6.1.

3.6 IIR FILTERS BASED ON TWO ALLPASS FILTERS

3.6.1 The Allpass Decomposition Theorem

A wide family of practical transfer functions including Butterworth, Chebyshev, and elliptic filters can be represented as

$$H_0(z) = \frac{A_0(z) + A_1(z)}{2}$$

where $A_0(z)$ and $A_1(z)$ are stable unit-magnitude allpass filters. This has been observed by a number of authors, for example, Fettweis [1974], Constantinides and Valenzuela [1982], Ansari and Liu [1985], Saramäki [1985], and Vaidyanathan, et al. [1986].

The following special case is particularly noteworthy: Let the transfer function $H_0(z)$ be Butterworth, Chebyshev or elliptic *lowpass*, with order N. Let n_0 and n_1 denote the orders of $A_0(z)$ and $A_1(z)$. Then the following things are true.

1. If N is odd, $A_0(z)$ and $A_1(z)$ have real coefficients, and $N = n_0 + n_1$.
2. If N is even, $A_0(z)$ and $A_1(z)$ have complex coefficients and $n_0 = n_1 = N/2$. In this case, the coefficients of $A_1(z)$ are conjugates of those of $A_0(z)$.

The proof of the first statement (odd N) follows from the theorem to be proved next. In this text, only odd N will be of interest, and will be used in Sec. 5.3 (alias-free IIR QMF banks). See Vaidyanathan et al. [1987] for details of even N, which will not be considered here. Also see Problem 3.20.

The fact that a sum of two allpass filters can give rise to good lowpass behavior might occassion an initial surprise. To appreciate the basic idea, recall that the allpass functions have frequency responses $A_0(e^{j\omega}) = e^{j\phi_0(\omega)}$ and $A_1(e^{j\omega}) = e^{j\phi_1(\omega)}$. Now the behavior of the magnitude of

$$H_0(e^{j\omega}) = \frac{e^{j\phi_0(\omega)} + e^{j\phi_1(\omega)}}{2}. \tag{3.6.1}$$

is governed by the phase difference $\phi_0(\omega) - \phi_1(\omega)$. From Sec. 3.4.1 we know that the phase responses of stable allpass filters are monotone decreasing functions. Figure 3.6-1 shows typical sketches of $\phi_0(\omega)$ and $\phi_1(\omega)$ which will ensure that $H_0(z)$ is a good lowpass filter. In the passband $\phi_0(\omega) \approx \phi_1(\omega)$ so that $|H_0(e^{j\omega})| \approx 1$. In the stopband $\phi_0(\omega) - \phi_1(\omega) \approx \pi$ so that $|H_0(e^{j\omega})| \approx 0$.

Thus, an appropriate behavior of relative phases of the two allpass filters can give rise to a good lowpass response. More generally, we will now state and prove the following result.

♠Theorem 3.6.1. Allpass decomposition. Let $H_0(z)$ and $H_1(z)$ be two Nth order bounded real (BR) transfer functions (Sec. 3.5) with irreducible rational forms $H_0(z) = P_0(z)/D(z)$ and $H_1(z) = P_1(z)/D(z)$ where,

$$P_0(z) = \sum_{n=0}^{N} p_{0,n} z^{-n}, \quad P_1(z) = \sum_{n=0}^{N} p_{1,n} z^{-n}, \quad D(z) = \sum_{n=0}^{N} d_n z^{-n}. \tag{3.6.2}$$

Suppose the following conditions are satisfied:

1. $P_0(z)$ is symmetric and $P_1(z)$ antisymmetric, that is,

$$p_{0,n} = p_{0,N-n}, \quad p_{1,n} = -p_{1,N-n}. \tag{3.6.3}$$

2. $H_0(z)$ and $H_1(z)$ are power complementary, satisfying (3.5.1b) with $c = 1$.

Then $H_0(z)$ and $H_1(z)$ can be expressed as

$$H_0(z) = \frac{A_0(z) + A_1(z)}{2}, \tag{3.6.4}$$

$$H_1(z) = \frac{A_0(z) - A_1(z)}{2}, \tag{3.6.5}$$

where $A_0(z)$ and $A_1(z)$ are stable real coefficient allpass functions

$$A_0(z) = \frac{z^{-n_0} \tilde{D}_0(z)}{D_0(z)}, \quad A_1(z) = \frac{z^{-n_1} \tilde{D}_1(z)}{D_1(z)}, \tag{3.6.6}$$

with orders n_0 and n_1, respectively. Moreover $N = n_0 + n_1$. ◇

Comments

1. The BR nature of $H_0(z)$ and $H_1(z)$ means that these are stable, that the coefficients $p_{0,n}, p_{1,n}$ and d_n are real and that the magnitudes on the unit circle are bounded by unity.
2. The allpass functions $A_0(z)$ and $A_1(z)$ have unit magnitude on the unit circle and their orders $A_0(z)$ and $A_1(z)$ add up to N.

3. Out of the N poles of $H_0(z)$, a subset of n_0 poles are assigned to $A_0(z)$ and the remaining n_1 poles assigned to $A_1(z)$. This partitioning of the poles of $H_0(z)$ *completely* determines its numerator. The zeros of $H_0(z)$ are, therefore, *not* independent parameters any more. The transfer function has only N degrees of freedom.
4. Figure 3.6-2 indicates a structure which implements the two transfer functions.

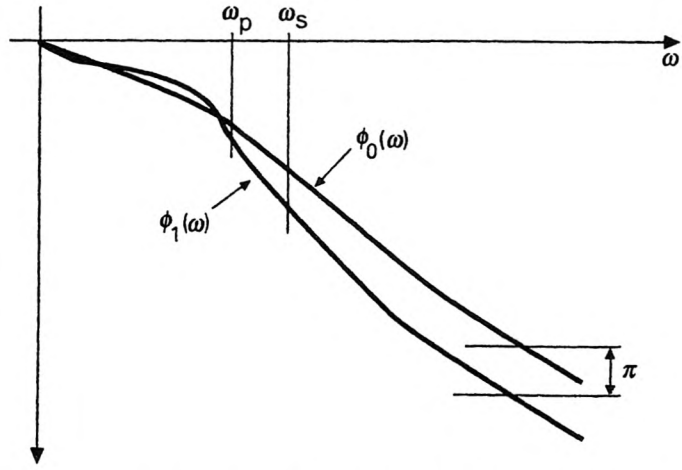

Figure 3.6-1 Demonstrating the phase responses of the two allpass functions.

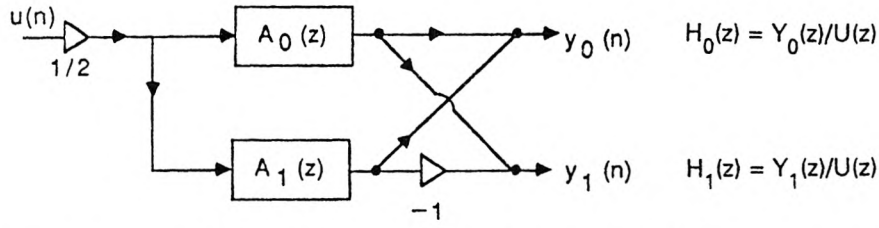

Figure 3.6-2 Implementing two transfer functions by adding and subtracting two allpass filters.

Proof of Theorem 3.6.1. First notice that (3.5.1b) can be rearranged as

$$\widetilde{P}_0(z)P_0(z) + \widetilde{P}_1(z)P_1(z) = \widetilde{D}(z)D(z), \tag{3.6.7}$$

since $c^2 = 1$. In view of (3.6.3) we have

$$\widetilde{P}_0(z) = z^N P_0(z), \quad \widetilde{P}_1(z) = -z^N P_1(z). \tag{3.6.8}$$

Substituting into (3.6.7) we obtain $P_0^2(z) - P_1^2(z) = z^{-N}\widetilde{D}(z)D(z)$, which can be rewritten as

$$\Big(P_0(z) + P_1(z)\Big)\Big(P_0(z) - P_1(z)\Big) = z^{-N}\widetilde{D}(z)D(z). \tag{3.6.9}$$

Notice that $P_0(z)-P_1(z) = z^{-N}\Big(\widetilde{P}_0(z)+\widetilde{P}_1(z)\Big)$ so that the zeros of $P_0(z)-P_1(z)$ are the reciprocal conjugates of those of $P_0(z)+P_1(z)$.

We know that the zeros of $D(z)$ are inside the unit circle so that those of $\widetilde{D}(z)$ are outside. So, none of the zeros of $P_0(z)+P_1(z)$ can be on the unit circle (from (3.6.9)). Let n_1 be the number of zeros of $P_0(z)+P_1(z)$ inside the unit circle. Then, there is a factor of $D(z)$, denote it $D_1(z)$, of order n_1 which is also a factor of $P_0(z)+P_1(z)$. Clearly, $P_0(z)+P_1(z)$ has $n_0 \triangleq N-n_1$ zeros outside the unit circle. As seen from (3.6.9) there is then a factor of $\widetilde{D}(z)$, say $\widetilde{D}_0(z)$, of order n_0 which is also a factor of $P_0(z)+P_1(z)$. Clearly $D_0(z)$ is a n_0th order factor of $D(z)$. Summarizing we can always write

$$P_0(z)+P_1(z) = \alpha D_1(z) z^{-n_0} \widetilde{D}_0(z), \tag{3.6.10}$$

where

$$D_0(z) = 1+\sum_{n=1}^{n_0} d_{0,n} z^{-n}, \quad \text{and} \quad D_1(z) = 1+\sum_{n=1}^{n_1} d_{1,n} z^{-n}, \tag{3.6.11}$$

are factors of $D(z)$, and α is a real nonzero constant.

As the orders of $D_0(z)$ and $D_1(z)$ add up to the order of $D(z)$, we get

$$D(z) = D_0(z) D_1(z). \tag{3.6.12}$$

By using (3.6.10) and (3.6.12) in (3.6.9) we obtain

$$P_0(z) - P_1(z) = \frac{1}{\alpha} D_0(z) z^{-n_1} \widetilde{D}_1(z). \tag{3.6.13}$$

But the symmetry relation (3.6.8) along with (3.6.10) also leads to this equation, with α in place of $1/\alpha$. This implies $\alpha = \pm 1$. We take $\alpha = 1$ (because the other choice $\alpha = -1$ does not change the magnitude responses of $H_0(z)$ and $H_1(z)$ anyway). Dividing both sides of (3.6.10) and (3.6.13) by $D(z)$ we finally arrive at

$$H_0(z)+H_1(z) = A_0(z), \quad H_0(z)-H_1(z) = A_1(z). \tag{3.6.14}$$

Rearranging (3.6.14), we therefore obtain (3.6.4) and (3.6.5). $\triangledown\triangledown\triangledown$

3.6.2 Elliptic, Butterworth, and Chebyshev Filters

Figure 3.6-3 shows the typical magnitude response of a fifth-order elliptic lowpass filter $H_0(z) = P_0(z)/D(z)$. The coefficients are known to be real, and the magnitude is bounded by unity so that $H_0(z)$ is BR. We know that all the zeros are on the unit circle. The zero at $\omega = \pi$ contributes to the factor $(1+z^{-1})$ and the complex conjugate pairs of zeros contribute to factors

of the form $(1 - 2z^{-1}\cos\omega_k + z^{-2})$. So, the numerator $P_0(z)$ is indeed a symmetric polynomial.

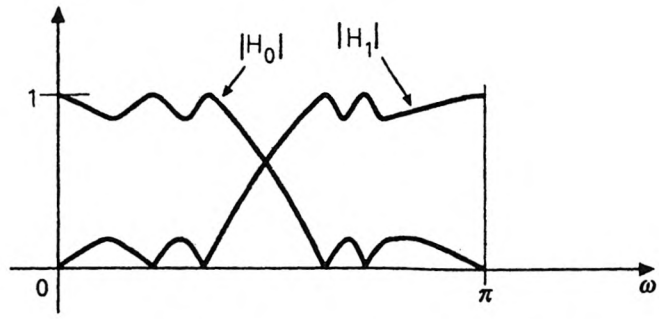

Figure 3.6-3 A fifth order elliptic lowpass filter, and its power complementary response.

The figure also shows the magnitude of the power complementary filter $H_1(z)$. Clearly, $|H_1(e^{j\omega})|$ is equal to zero at frequencies where, $|H_0(e^{j\omega})|$ takes the maximum value of unity. $|H_1(e^{j\omega})|$ has one zero at $\omega = 0$ and two complex conjugate pairs of zeros on the unit circle so that all the zeros are on the unit circle again. The zero at $\omega = 0$, however, contributes to an *antisymmetric factor* $(1 - z^{-1})$. As a result, the numerator $P_1(z)$ of $H_1(z)$ is antisymmetric. Summarizing, $H_0(z)$ has a symmetric numerator and $H_1(z)$ has an antisymmetric numerator.

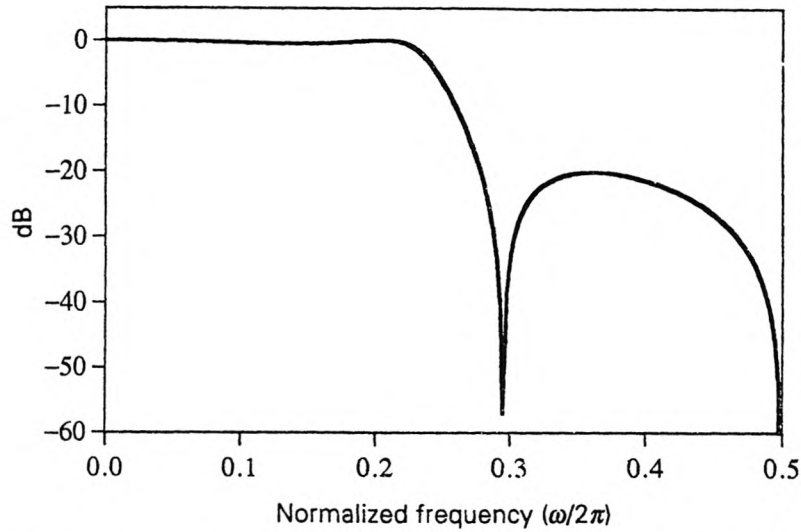

Figure 3.6-4 Example 3.6.1. Magnitude response of a 3rd order elliptic filter.

More generally, if $H_0(z)$ represents an *odd order lowpass* Butterworth, Chebyshev or elliptic filter, the above conclusions remain valid. That is, the

numerator of $H_0(z)$ is symmetric and that of $H_1(z)$ is antisymmetric. We can, therefore, apply Theorem 3.6.1 to conclude that $H_0(z)$ and $H_1(z)$ can be expressed as in (3.6.4) and (3.6.5).

Example 3.6.1

Consider the third order elliptic lowpass filter

$$H_0(z) = \frac{0.23179 + 0.36021z^{-1} + 0.36021z^{-2} + 0.23179z^{-3}}{1 - 0.38409z^{-1} + 0.70390z^{-2} - 0.13581z^{-3}} \qquad (3.6.15)$$

whose magnitude response is shown in Fig. 3.6-4. The reader can verify that $H_0(z)$ can be expressed as

$$H_0(z) = 0.5\left[\underbrace{\frac{-0.20356 + z^{-1}}{1 - 0.20356z^{-1}}}_{A_0(z)} + \underbrace{\frac{0.66715 - 0.18053z^{-1} + z^{-2}}{1 - 0.18053z^{-1} + 0.66715z^{-2}}}_{A_1(z)}\right].$$

Evidently $A_0(z)$ and $A_1(z)$ indicated above are unit-magnitude allpass.

Efficiency of the Allpass Based Structure

The cost of the implementation of Fig. 3.6-2 (say an elliptic filter) is equal to the cost of the two allpass filters plus the two adders. We know from Sec. 3.4.3 that a real coefficient allpass filter of order n_k can be implemented with n_k multipliers. So, the structure requires only $n_0 + n_1 = N$ multipliers. For this cost, we get two filters $H_0(z)$ and $H_1(z)$, that is, we require $N/2$ multipliers per filter! In contrast, a direct form implementation of a single elliptic filter would require as many as $1.5N$ multipliers (even after taking numerator symmetry into account)!

The Pole Interlace Property

Given an odd order elliptic transfer function $H_0(z) = P_0(z)/D(z)$, what is the procedure to identify the allpass functions $A_0(z)$ and $A_1(z)$? One method would be to identify $P_1(z)$ using (3.6.7), and compute the zeros of $P_0(z) + P_1(z)$. The zeros inside the unit circle determine $D_1(z)$, and those outside are used to determine $D_0(z)$. The allpass functions can then be found from (3.6.6).

There exists a simpler procedure, whenever the zeros of $D(z)$ [poles of $H_0(z)$] are known. Let the poles of $H_0(z)$ be $z_0, z_1, \ldots$, with pole angles $\theta_0, \theta_1, \ldots$ Let the numbering of poles be such that $\theta_0 < \theta_1 < \ldots$. Then the poles of $A_0(z)$ are given by z_{2k} and those of $A_1(z)$ by z_{2k+1}. This is called the *pole interlace property* [Gazsi, 1985]. Using this we can identify the allpass functions as demonstrated in Fig. 3.6-5.

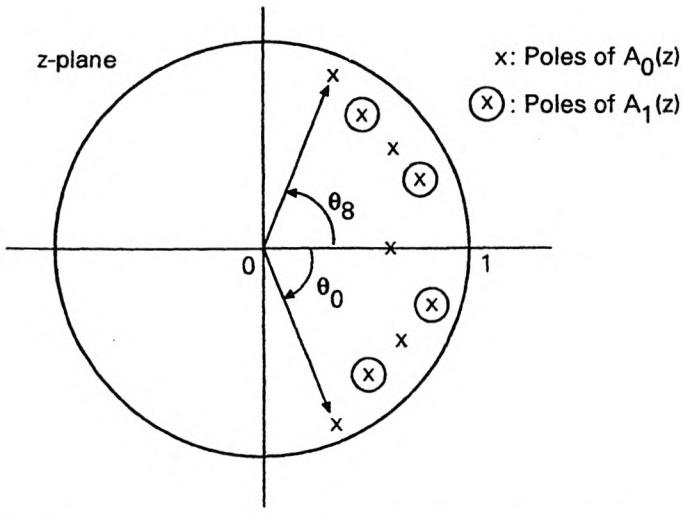

Figure 3.6-5 Demonstration of interlace property. The nine poles of $H_0(z)$ are split into those of $A_0(z)$ and $A_1(z)$ as indicated.

Case When N is Even

What happens if the filter has even order? Consider a sixth order elliptic lowpass filter $H_0(z) = P_0(z)/D(z)$ with response as shown in Fig. 3.6-6. In the region $0 \leq \omega \leq \pi$, there are three zeros. Thus we have three complex conjugate pairs of zeros, giving rise to three factors of the form $(1 - 2z^{-1}\cos\omega_k + z^{-2})$ for the numerator $P_0(z)$. This numerator, therefore, is symmetric.

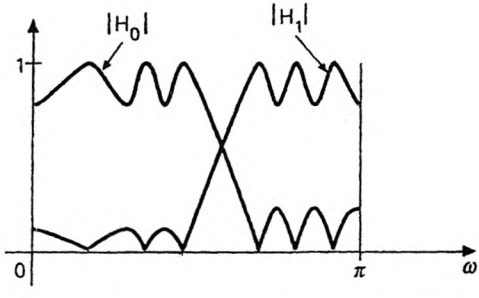

Figure 3.6-6 A sixth order elliptic lowpass filter and its power complementary response.

Now consider the power complementary response $|H_1(e^{j\omega})|$ which is also shown in the figure. This is zero whenever $|H_0(e^{j\omega})|$ is unity. Since $|H_0(e^{j\omega})|$ does *not* have a maximum at $\omega = 0$, we conclude that $|H_1(e^{j\omega})| \neq 0$ at $\omega = 0$. So the numerator $P_1(z)$ of $H_1(z)$ does not have the factor $(1 - z^{-1})$. In fact $P_1(z)$ has three factors of the form $(1 - 2z^{-1}\cos\theta_k + z^{-2})$ because it also has three pairs of complex conjugate zeros on the unit circle. As a result $P_1(z)$ is symmetric rather than antisymmetric. More generally whenever $H_0(z)$ is

a Butterworth, Chebyshev or elliptic lowpass filter of even order, the above conclusion remains true. That is, the numerators of $H_0(z)$ and $H_1(z)$ are both symmetric. So, the conditions of Theorem 3.6.1 are not satisfied.

In this case it can be shown [Vaidyanathan, et. al., 1987] that we can still express $H_0(z)$ as $0.5[A_0(z)+A_1(z)]$, where $A_0(z)$ and $A_1(z)$ are complex-coefficient allpass filters, and the coefficients of $A_1(z)$ are conjugates of those of $A_0(z)$. Finally, note that if $H_0(z)$ is bandpass or bandstop, then it can often be implemented in terms of real allpass filters, even if its order is even. (Example: start from an odd order elliptic lowpass filter and replace z with z^2 or $-z^2$.)

TABLE 3.7.1 Comparison of four techniques for lowpass filter design. The specifications are $\omega_p = 0.15\pi$, $\omega_S = 0.20\pi$, $\delta_1 = 0.01$ and $\delta_2 = 0.001$.

Method	IIR elliptic	IIR Butterworth	FIR equiripple	FIR Kaiser window
Special features	Optimal in minimax sense	Maximally flat at $\omega = 0, \pi$	Linear phase. Also optimal in minimax sense	Linear phase. Very easy to design
Required order N	7	28	101	146
Complexity of Implementation	11 mul* 14 add (direct form)	28 mul, 56 add (direct form)	51 mul, 101 add	74 mul, 146 add

* 7 mul and 22 add, if the allpass based structure is used (with one-multiplier lattice sections).

3.7 CONCLUDING REMARKS

In Sec. 3.1 to 3.3 we reviewed many techniques for digital filter design. A summary and comparison of many of the earlier methods can be found in Rabiner and Gold [1975]. In Table 3.7.1 we have compared the filter orders and computational complexities of several methods, for a given set of specifications on the magnitude response. It is clear that the IIR elliptic design is the least expensive, but it introduces phase distortion. The FIR filters, on the other hand, have exact linear phase, but are more expensive. As explained at the beginning of Sec. 3.3, the complexity in terms of multiplications and additions is not always a fair measure of comparison. One should take into account the architecture of the implementation and, if possible, use more efficient FIR implementations (e.g., multistage implementations, Sec. 4.4).

The following Chapters will show that in the context of multirate signal

processing, some of the methods we described are particularly suitable, for example, window techniques, eigenfilter techniques and IIR elliptic designs. For this reason, we have elaborated them in this chapter. We will see later (Sec. 5.3) that IIR filters based on a sum of two allpass functions (Sec. 3.6) are particulary useful in filter bank designs.

PROBLEMS

3.1. Let $H(z) = \sum_{n=0}^{N} h(n)z^{-n}$ be a Type 1 linear phase FIR filter and let $G(z) = \sum_{n=0}^{N} g(n)z^{-n}$ with

$$g(n) = (-1)^M \delta(n - M) - (-1)^n h(n), M = N/2. \qquad (P3.1)$$

Prove that $G(z)$ is also a linear phase filter. Assuming that the amplitude response of $H(z)$ is as in Fig. 3.2-7, give a qualitative plot of the amplitude response of $G(z)$. Clearly indicate the bandedges and ripple sizes in terms of the known quantities $\omega_p, \omega_S, \delta_1, \delta_2$. What sort of filter is $G(z)$ (i.e., lowpass or highpass or ...)?

3.2. Let $G(z)$ be an ideal transfer function such that $G(e^{j\omega}) = 1$ for $0 \leq |\omega| \leq \pi/4$ and zero elsewhere.

a) Consider the new system $H(z) = G(z^2)$. Plot $|H(e^{j\omega})|$ for $0 \leq \omega \leq \pi$.

b) Consider the system constructed according to the following flowgraph:

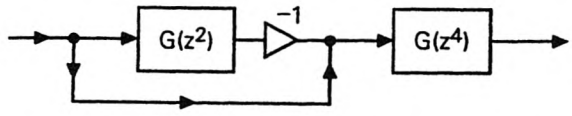

Figure P3-2

Plot the magnitude response of this new system for $0 \leq \omega \leq \pi$. What kind of a filter is this (i.e., lowpass or highpass or ...)?

3.3. Let $H(z)$ and $\widehat{H}(z)$ be two lowpass filters. Let δ_1 and δ_2 be the peak passband and stopband ripples for $H(z)$, and $\widehat{\delta}_1$ and $\widehat{\delta}_2$ the corresponding ripples for $\widehat{H}(z)$. Assume that all these ripples are very small compared to unity. The cascaded filter $H(z)\widehat{H}(z)$ is clearly lowpass. Show that its peak passband ripple $\leq \delta_1 + \widehat{\delta}_1$, and peak stopband ripple $\leq \max(\delta_2, \widehat{\delta}_2)$.

3.4. Consider a zero phase FIR lowpass filter $H(z)$ with the frequency response shown in Fig. P3-4(a). Here δ_1 and δ_2 represent the peak ripple sizes. Our aim is to generate a better filter by making multiple use of the filter $H(z)$. In Fig. P3-4(b)–(d) we have shown three structures which attempt to do this.

a) In each case give a qualitative plot of the amplitude response and verify that the resulting filter continues to be lowpass with (nearly) same bandedges as $H(z)$.

b) In each case find the peak to peak passband and stopband ripple. Assuming $\delta_1 = 0.0025$ and $\delta_2 = 0.002$, compute all these ripple sizes, and present them in the form of a neat table.

c) If you wish to design a filter which is better than $H(z)$ in the passband, which of the three methods would you choose?

d) If you wish to design a filter which is better than $H(z)$ in the stopband, which of the three methods would you choose?

e) If you wish to design a filter which is better than $H(z)$ in the passband *and* stopband, which of the three methods would you choose?

f) Show how these three structures should be modified if $H(z)$ is not zero-phase, but Type 1 linear-phase with order N (with Fig. P3-4(a) representing the amplitude response).

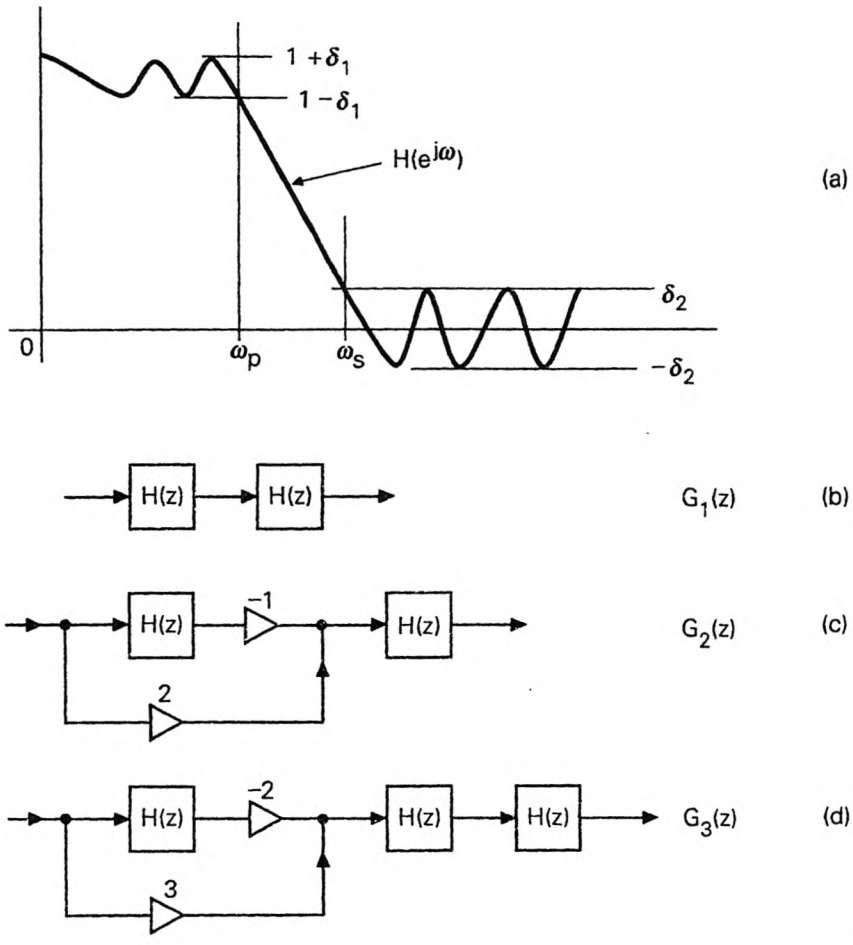

Figure P3-4

Note. You can assume that δ_1 and δ_2 are 'sufficiently small' in order to make *wise* engineering simplification of your expressions.

3.5. Let

$$F(\omega) = \sum_{k=-\infty}^{\infty} f(k)\Phi_k(\omega), \qquad (P3.5a)$$

where $\Phi_k(\omega)$ is a set of orthonormal functions in the range $a \leq \omega < b$, that is, $\int_a^b \Phi_k(\omega)\Phi_m^*(\omega)d\omega = \delta(k-m)$. In other words, $F(\omega)$ is a linear combination of an orthonormal set of basis functions $\Phi_k(\omega)$ in the interval $a \leq \omega < b$. The most common example is when

$$\Phi_k(\omega) = e^{jk\omega}/\sqrt{2\pi}, \quad a = 0, \quad b = 2\pi. \qquad (P3.5b)$$

In this case, the above summation reduces to the familiar Fourier transform of the sequence $f(k)$.

a) Suppose we wish to approximate $F(\omega)$ with the finite summation

$$F_M(\omega) = \sum_{k=-M}^{M} \hat{f}(k)\Phi_k(\omega) \qquad (P3.5c)$$

in the region $a \leq \omega < b$. We wish the approximation to be "best in the least squares sense", that is, $e \triangleq \int_a^b |F(\omega) - F_M(\omega)|^2 d\omega$ must be minimized. Show that the choice $\hat{f}(k) = f(k), -M \leq k \leq M$ achieves this.

b) With $\hat{f}(k) = f(k)$, what is the minimized error e? Simplify as best as you can.

c) Consider the window design procedure for zero-phase FIR lowpass filters. Show that, if we use the rectangular window, the resulting filter is optimal in the least square sense.

3.6. In Sec. 3.2.2 we stated that the matrix **P** in the real-coefficient optimal window design problem is real, symmetric, positive definite and Toeplitz, with a unique eigenvector (up to scale) for each eigenvalue. In this problem we use some or all of these properties to derive two useful conclusions.

a) Prove that the optimal window is symmetric, that is, $v(n) = v(N-n)$. (*Note:* You can ignore the possibility of an antisymmetric window, as that would imply a zero at $\omega = 0$, which in turn conflicts the energy maximization requirement.)

b) Prove that the z-transform $V(z)$ of the optimal window $v(n)$ has all zeros on the unit circle.

Note: Part (b) was stated in text without proof. Evidently (b) implies (a). However, an independent proof of (a) is easier than (b).

3.7. Shown in the following figure is an example of a typical bandpass response.

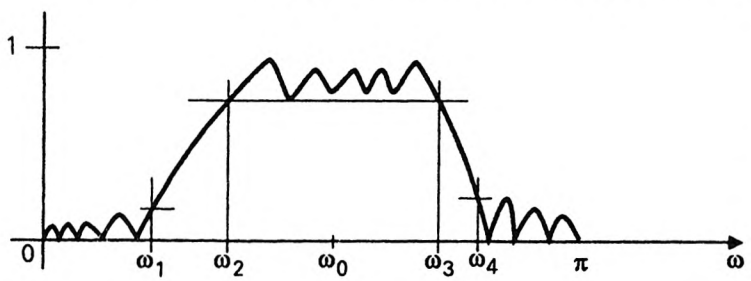

Figure P3-7

Here ω_0 is the center (or reference) frequency and $\omega_1, \omega_2, \omega_3, \omega_4$ represent the bandedges. In Sec. 3.2.3 we described how to design lowpass eigenfilters, which are optimal in the sense of minimizing the stopband and passband errors in a certain least square sense. Describe how this can be extended for the design of bandpass filters of the above form. Assume the filter to be Type 1 linear phase FIR for simplicity.

3.8. Consider the method of Sec. 3.2.3 for design of lowpass eigenfilters. It is clear from the definition of E_S that it cannot be zero as long as $\omega_S \neq \pi$. Similarly E_p cannot be negative. Based on these physical considerations prove that the Hermitian matrices $\mathbf{P}$ and $\mathbf{R}$ are positive definite (as long as α is restricted to $0 < \alpha < 1$).

3.9. Let $H(z)$ be a Type 3 linear phase FIR filter, with passband in the range $0 < \omega_1 \leq \omega \leq \omega_2 < \pi$. Suppose $x(n)$ is a real signal with no energy outside the passband of $H(z)$. It is obvious that the output $y(n)$ is real because $h(n)$ and $x(n)$ are real. However, we also know that $H(e^{j\omega}) = ce^{-j\omega N/2}H_R(\omega)$, where c is a *complex* constant ($c = j$). Assuming that $H(e^{j\omega})$ has a "good passband", that is, very small passband ripple, do you still think that $y(n)$ has the form $y(n) \approx \alpha x(n - M)$ where α is a real constant? (*Hint:* Try $x(n) = \cos(\omega_0 n + \theta)$ where ω_0 belongs to the passband and θ is real.)

3.10. Find the coefficients of a second order digital lowpass Butterworth filter with 3 dB point at $\omega = 0.2\pi$.

3.11. Consider the Butterworth response (3.3.6). Show that the first $2N - 1$ derivatives are zero at $\Omega = 0$.

3.12. Suppose we wish to transform an analog filter $H_a(s)$ into digital filter $H(z)$. Assume that the following transformation has been used: $s = 1 - z^{-1}$. This is called the backward difference approach. (The motivation for this substitution is that s represents differentiation and $1 - z^{-1}$ represents a first difference.)

a) Suppose $H_a(s)$ has all poles in $\mathrm{Re}[s] < 0$. Does it necessarily mean that $H(z)$ has all poles inside the unit circle?

b) Suppose $H(z)$ has all poles inside the unit circle. Does it mean that $H_a(s)$ has all poles in $\mathrm{Re}[s] < 0$?

c) Instead of the above mapping assume that we use the mapping $s = z - 1$ (forward difference approach). Repeat parts (a) and (b).

3.13. In this problem we shall give an overview of Chebyshev polynomials. Recall that the hyperbolic cosine function is defined as $\cosh\theta = (e^{\theta} + e^{-\theta})/2$. Let us denote this as x, that is,

$$\cosh\theta = x = \frac{e^{\theta} + e^{-\theta}}{2}. \qquad (P3.13a)$$

Here θ could be real or complex. If x is real then either θ is real or e^{θ} is the conjugate of $e^{-\theta}$.

a) For real θ show that $x \geq 1$. Also justify that $-1 \leq x \leq 1$ if, and only if, $\theta = j\omega$ where ω is real.

b) Show that

$$\cosh\big((N \pm 1)\theta\big) = \cosh(N\theta)\cosh\theta \pm \sinh(N\theta)\sinh\theta. \qquad (P3.13b)$$

Hence, prove the recursion

$$C_{N+1}(x) = 2xC_N(x) - C_{N-1}(x) \qquad (P3.13c)$$

where $C_N(x) = \cosh(N\theta) = \cosh(N\cosh^{-1}x)$. For example $C_1(x) = \cosh\theta = x$.

c) Evidently, $C_0(x) = 1$ and $C_1(x) = x$. Prove by use of the recursion (P3.13c) that $C_N(x)$ is a polynomial for any x. $C_N(x)$ is called the Nth order Chebyshev polynomial. Give qualitative plots of $C_N(x)$ for $N = 0, 1, 2, 3, 4$.

d) Prove that $C_N(x)$ is an even polynomial (i.e., has only even powers of x) for even N, and odd polynomial for odd N. Also show that $C_N(1) = 1$ and that the highest power x^N has coefficient 2^{N-1} for $N \geq 1$.

e) Show that all the N zeros of $C_N(x)$ are real and lie in the range $-1 < x < 1$. (*Hint.* $C_N(x) = \cosh(N\theta) = \cos(N\omega)$ for $\theta = j\omega$, ω real.) So, in the region $|x| > 1$, the behavior is monotone as demonstrated below.

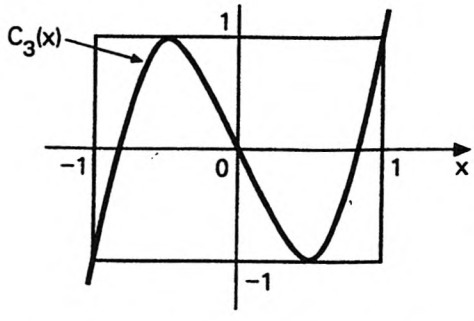

Figure P3-13

f) Let $C_N(x) = c_N(0) + c_N(1)x + \ldots c_N(N)x^N$. Let $P(x) = p(0) + p(1)x + \ldots + p(N)x^N$ be some real coefficient polynomial with $p(N) = c_N(N)$. Prove that

$$\max_{-1 \leq x \leq 1} |P(x)|^2 \geq \max_{-1 \leq x \leq 1} |C_N(x)|^2. \qquad (P3.13d)$$

This shows that among all polynomials of order N with highest coefficient equal to that of $C_N(x)$, the Chebyshev polynomial has the smallest peak value in $-1 \leq x \leq 1$. So, the polynomial has the minimax property (i.e., *max*imum magnitude in $-1 \leq x \leq 1$ is *min*imized).

3.14. Consider the response

$$|H_a(j\Omega)|^2 = \frac{1}{1 + \epsilon^2 C_N^2(\Omega/\Omega_p)}, \qquad (P3.14a)$$

where $\Omega_p > 0$. This is called the *Chebyshev response* and a stable tranfer function $H_a(s)$ with this response is called a *Chebyshev filter.*

a) Justify that the magnitude response has the behavior shown in Fig. P3-14, when $N = 7$. The quantity Ω_p is the passband edge, and ϵ directly controls the passband ripple size. The passband is equiripple. All the $2N$ zeros of (P3.14a) are at $\Omega = \infty$.

b) By making wise engineering assumptions show that the required order N (for a given set of specifications) can be estimated from

$$N = \frac{A_S + 20\log_{10}(1/\epsilon) + 6.02}{8.686\cosh^{-1}(\Omega_S/\Omega_p)}. \qquad (P3.14b)$$

c) Plot the response $|G_a(j\Omega)|^2 = 1 - |H_a(j/\Omega)|^2$. This should be lowpass with equiripple stopband and monotone passband. A stable transfer function $G_a(s)$ with this behavior is called an *inverse Chebyshev filter.*

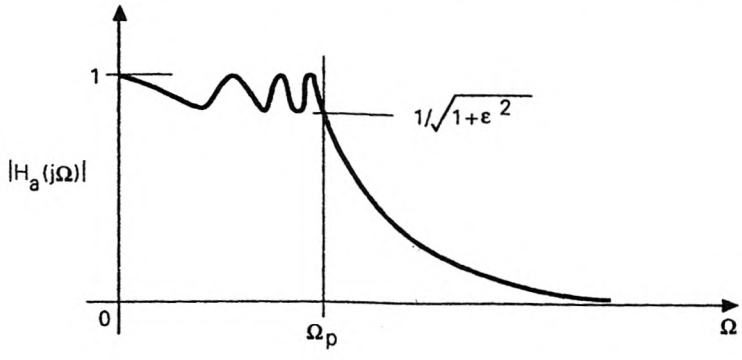

Figure P3-14

d) Suppose $H(z)$ is obtained by use of bilinear transformation on $H_a(s)$. Specify any special feature that the numerator of $H(z)$ might have.

3.15. For an analog elliptic lowpass filter $H_a(s)$, assume that the bandedges are related as $\Omega_p\Omega_S = 1$. Let $G_a(s)$ be a stable filter such that $|G_a(j\Omega)|^2 = 1 - |H_a(j/\Omega)|^2$.

a) Qualitatively plot the responses $|H_a(j\Omega)|^2$ and $|G_a(j\Omega)|^2$ for $N = 5$.

b) Give a simple argument to justify that the reflection and transmission zeros (α_k's and β_k's in Fig. 3.3-2) satisfy $\alpha_k = 1/\beta_k$.

3.16. Suppose we wish to design a digital lowpass filter with specifications ω_p, ω_S, δ_1 and δ_2 as in Table 3.7.1. Verify that the required order N is as in the table, for the two FIR cases and for the IIR Butterworth case.

3.17. In the continuous-time world a rational transfer function $G(s)$ of degree $N > 0$ with real coefficients is said to be a reactance if it satisfies the following two properties: (a) $\mathrm{Re}[G(j\Omega)] = 0$ for all frequencies Ω and (b) $\mathrm{Re}[G(s)] > 0$ for all s in the right half plane, that is, for all s such that $\mathrm{Re}[s] > 0$. Now define a discrete-time transfer function $H(z)$ as follows:

$$H(z) = \left.\frac{1 - G(s)}{1 + G(s)}\right|_{s=(1-z^{-1})/(1+z^{-1})} \qquad (P3.17)$$

Show then that $H(z)$ represents an allpass function with all poles strictly inside the unit circle. (*Note.* It turns out that $G(s)$ is a reactance if and only if it is the input impedance of a lossless electrical network (LC network with positive elements). This establishes the link between digital allpass functions and continuous-time LC networks.)

3.18. Allpass functions have played an important role in continuous-time filter theory also. Consider a causal system with transfer function

$$H(s) = \frac{-s - a^*}{s - a}. \qquad (P3.18)$$

Here a and $-a^*$ are the pole and zero respectively.

a) Prove that this is allpass, that is, $|H(j\Omega)| = 1$.

b) Assuming $\mathrm{Re}[a] < 0$ (that is, $H(s)$ stable) prove by explicitly writing down $|H(s)|$ that $|H(s)| < 1$ for $\mathrm{Re}[s] > 0$ and $|H(s)| > 1$ for $\mathrm{Re}[s] < 0$.

c) Consider the following pole-zero diagram for $H(s)$.

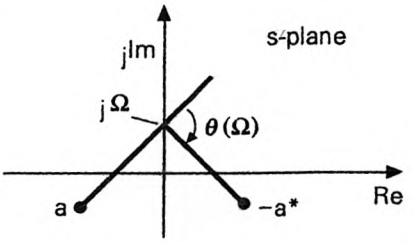

Figure P3-18

Show that the phase response at frequency Ω is the angle $\theta(\Omega)$ indicated in the figure. This shows, essentially by inspection, that this is a monotone decreasing function of Ω.

An Nth order unit-magnitude allpass function is a product of N first order functions of the form (P3.18). So if all the poles are in the left half plane, properties (b) and (c) continue to hold. Since any discrete-time stable allpass function can be derived from a continuous-time counterpart using bilinear transform, this gives a second proof of these same properties for the discrete-time case.

3.19. Consider Fig. 3.4-7, and assume $|k_m| < 1$. Assume $G_{m-1}(z)$ has all poles inside the unit circle, and let $|G_{m-1}(e^{j\omega})| = 1$ for all ω.

a) Show that $|G_m(e^{j\omega})| = 1$ for all ω, and that all its poles are inside the unit circle.

b) Consider the lattice structure of Fig. 3.4-8. Let $|G_0| = 1$, and $|k_m| < 1$ for all m. Show that the transfer function $G_N(z)$ has all poles inside the unit circle, and that $|G_N(e^{j\omega})| = 1$.

3.20. *Generalization of allpass decomposition.* Let $H_0(z) = P_0(z)/D(z)$ and $H_1(z) = P_1(z)/D(z)$ be two stable transfer functions (with possibly complex coefficients) of order N with

$$P_0(z) = \sum_{n=0}^{N} p_{0,n} z^{-n}, \quad P_1(z) = \sum_{n=0}^{N} p_{1,n} z^{-n}, \quad D(z) = 1 + \sum_{n=1}^{N} d_n z^{-n}.$$

Assume that the following properties are true. (a) $P_0(z)$ is Hermitian, (b) $P_1(z)$ is generalized-Hermitian (i.e., $\widetilde{P}_1(z) = cz^N P_1(z)$ for some c with $|c| = 1$) and (c) $|H_0(e^{j\omega})|^2 + |H_1(e^{j\omega})|^2 = 1$, (i.e., power complementarity). Prove that $H_0(z)$ and $H_1(z)$ can be expressed as

$$H_0(z) = \frac{\beta A_0(z) + \beta^* A_1(z)}{2}, \quad H_1(z) = d\frac{\beta A_0(z) - \beta^* A_1(z)}{2},$$

where $A_0(z)$ and $A_1(z)$ are stable unit-magnitude allpass of orders n_0 and n_1 with $n_0 + n_1 = N$ and where $|\beta| = |d| = 1$.

3.21. Let $G(z) = A_0(z) + A_1(z)$, where $A_0(z)$ and $A_1(z)$ are allpass. Show that $G(z)$ is allpass if, and only if, $A_1(z) = cA_0(z)$ for some constant c.